DRIVERS OF SUB-SEASONAL TO INTERANNUAL SHORELINE

CHANGE AT SUNSET STATE BEACH IN MONTEREY BAY, CA

—————————

A Thesis

Presented to the

Faculty of

Moss Landing Marine Laboratories

California State University Monterey Bay

—————————

In Partial Fulfillment

of the Requirements for the Degree

Master of Science

in

Marine Science

—————————

by

Miya Pavlock

Term Completed: Spring 2020

CALIFORNIA STATE UNIVERSITY MONTEREY BAY

The Undersigned Faculty Committee Approves the

Thesis of Miya Pavlock:

DRIVERS OF SUB-SEASONAL TO INTERANNUAL SHORELINE CHANGE AT

SUNSET STATE BEACH IN MONTEREY BAY, CA

_____

Tom Connolly, Chair
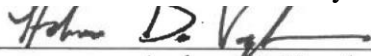Moss Landing Marine Laboratories

_____

Ivano Aiello
Moss Landing Marine Laboratories

_____

Rikk Kvitek
Cali ornia State University Monterey Bay

Andrew DeVogelaere
NOAA's Monterey Bay National Marine Sanctuary

_____

Shawn Harrison
US Naval Research Laboratory - Stennis Space Center

_____

Kris Roney, Dean
Associate VP for Academic Programs and Dean of Undergraduate and Graduate Studies

11 May 2020
_____

Approval Date

ABSTRACT

Drivers of Sub-Seasonal to Interannual Shoreline Change at Sunset
State Beach in Monterey Bay, CA
by
Miya Pavlock
Master of Science in Marine Science
California State University Monterey Bay, 2020

Expectations of future change call for a thorough understanding of short- and long-time scale processes that impact sandy beaches, as well as tests of coastal change models in a variety of coastal settings. However, existing shoreline change models have primarily been developed and tested in open coast environments. Therefore, this study takes place in the northern Monterey Bay where we investigate the effects of headland sheltering and complex inner shelf bathymetry on shoreline change at a sandy dune-backed beach, fronted by a submarine canyon system. Twenty months of half-hourly video imagery were used to build a high-resolution time series of shoreline and sandbar positions at Sunset State Beach from September 2017 to May 2019. Past studies have shown that high magnitudes of winter shoreline erosion in the Monterey Bay occur during El Niño periods, when storm tracks over the northeast Pacific Ocean shift southward. This motivated the assessment of interannual shoreline variability by extending the shoreline time series back to September 2014 with biannual in-situ surveys.

According to the video derived observations, the shoreline varied by approximately 60 meters while the sandbar varied by approximately 100 meters in the cross-shore direction. Winter shoreline erosion began when nearshore significant wave heights exceeded the 95th percentile (1.7m), and a greater magnitude of shoreline erosion occurred with higher average winter wave energy. Shoreline accretion appeared to be aided by the sandbar, which acted as a source of sediment in the early summer months of 2018. The influence of wave energy and direction on shoreline change was tested using an equilibrium shoreline change model and an alongshore sediment transport model. Shoreline change at Sunset State Beach depended primarily on wave energy, the root-mean-squared error (RMSE) of the equilibrium model alone was 6.4m. The addition of alongshore sediment transport to overall shoreline change resulted in a modest RMSE reduction to 5.6m, but equilibrium model parameters did not change significantly. According to the biannual time series of shoreline observations, high magnitudes of shoreline erosion can also occur during non- El Niño periods, due to westerly waves that bypass the Santa Cruz headlands and expose the northern Monterey Bay to wave attack. The accuracy of the shoreline change models used in this study was limited by annual variability in the summer shoreline position, motivating future investigations of temporally variable alongshore sediment supply. The results suggest that rather than relying on predictions of an El Niño index to predict shoreline change, predictions of the direction of storm tracks over the northeast Pacific Ocean could more accurately inform shoreline change predictions at the study site and in similar environments.

TABLE OF CONTENTS

LIST OF TABLES

LIST OF FIGURES

ACKNOWLEDGEMENTS

SECTION 1

INTRODUCTION

The changing wave climate in combination with sea level rise is likely to increase coastal erosion rates and threaten the economic, social, and cultural value of sandy coasts (Mentaschi, et al., 2017; Neumann et al., 2014; Semedo et al., 2013; Zhang et al., 2004). Therefore, projections of shoreline change are an increasingly useful tool for coastal managers to enact effective coastal management plans. Accurate projections, however, require a thorough understanding of the physical drivers of coastal change, as well as observations capable of resolving short and long timescale processes that impact sandy coasts. Expectations of future change emphasize the need for efficient data collection methods and tests of existing shoreline change models to assess their utility in a variety of coastal settings.

Shoreline change is largely driven by waves which are affected on various timescales by controls such as headland sheltering, complex bathymetry, and nearshore sandbars (Hapke et al., 2016; Harrison et al., 2017; Stive et al., 2002). Headlands can shelter or expose certain stretches of beach depending on the shoreline orientation and direction of incoming waves. Complex inner shelf and nearshore bathymetry, such as that of submarine canyon systems, can refract or steer larger waves and cause alongshore variations in wave height (Munk & Traylor, 1947). In the nearshore, sandbars dissipate wave energy as shore-normal incident waves drive sediment transport in the cross-shore direction (Hoefel & Elgar, 2003; Lippmann & Holman, 1989; Wright & Short, 1984).

Waves drive shoreline change by mobilizing sand across and alongshore according to their magnitude and direction (Komar & Inman, 1970; Wright & Short, 1984). The magnitude of shoreline migration due to sediment transport processes can be estimated with simple models forced with wave energy and direction (e.g. Yates et al., 2009; USACE 1984). Cross-shore sediment transport occurs when waves approach perpendicular to shore, and alongshore sediment transport occurs when gradients in alongshore wave conditions develop. Simple shoreline change models have been combined to forecast expected change coastal but have primarily been tested in open coast environments (e.g. Vitousek et al., 2017).

At open coast sandy beaches many studies have found that the shoreline position constantly adjusts toward a state of equilibrium with wave conditions, typically eroding rapidly during high energy wave conditions and accreting gradually during low energy wave conditions (Davidson et al., 2013; Splinter et al., 2014; Yates et al., 2009). Shoreline erosion is generally accompanied by offshore sandbar migration, and shoreline accretion is accompanied by onshore sandbar migration. High energy waves during storms bring the most erosive waves to coastal areas on the order of hours to days, which is a difficult timescale to observe with in-situ surveying methods. The rise of video remote sensing has allowed for observations of morphologic characteristics before, during, and after storms leading to investigations of the drivers of storm erosion and post storm accretion or recovery (Angnuureng et al., 2017; Blossier et al., 2017; Burvingt et al., 2017; Coco et al., 2014; Phillips et al., 2017; Senechal et al., 2015; Splinter et al., 2014). Angnuureng et al. (2017) for example, suggest that storm driven shoreline erosion is controlled by the wave energy of present and previous storms, and post storm recovery is primarily modulated by sandbar location at a sandy barred beach in France. We therefore use automated video remote sensing in the present study as an efficient method to gather observations of shoreline and sandbar location capable of resolving the impacts of individual storm events.

The present study takes place in Monterey Bay, where we investigate the effects of headland sheltering and complex inner shelf bathymetry on shoreline change at a sandy dune-backed beach, fronted by a submarine canyon system. The objectives of this study are twofold: 1) to define the relationships between shoreline and sandbar positions with wave conditions at the study site and 2) to test the drivers of shoreline change with simple shoreline change models. First, we explore the ability of the sandbar to dissipate wave energy and buffer the shoreline to delay winter erosion by quantifying the relationships between shoreline and sandbar positions with wave conditions. Later, shoreline change due to cross- and alongshore sediment transport processes are estimated with simple models. If wave energy is a primary driver of shoreline change at the study site, it was expected that a simple equilibrium shoreline change model would yield accurate predictions of shoreline position based on hourly changes in wave energy. The high elevation dune provides an ideal perspective for automated video monitoring which is used here in the Monterey Bay to map shoreline and sandbar positions.

1a. Study Area

Monterey Bay in Central California is located approximately 150km south of San Francisco and is characterized by sea cliffs and eroding pocket beaches in Santa Cruz, low-lying rocky shores in Monterey, and long stretches of sandy dune-backed beaches in between (Figure 1). River input and the erosion of coastal sea cliffs and dunes act as major sources of sediment in the greater Monterey Bay, while offshore sediment transport, losses to the Monterey submarine canyon head near Moss Landing, and sand mining in the southern Monterey Bay act as major sinks (Griggs & Patsch, 2007). The Monterey submarine canyon system can refract waves as they approach from offshore and promote alongshore wave energy gradients, especially apparent with the presence of extreme waves approaching from the west (Erikson et al., 2014). The tidal regime is semidiurnal with a maximum range of 2m.

The present study site, Sunset State Beach, is in the northern Monterey Bay and is sheltered from northwest swell originating in the northern Pacific Ocean by the Santa Cruz headlands, most of the year (Figure 1). Sunset State Beach was selected for this study because it is backed by the highest dune in the Monterey Bay, that provides an ideal viewpoint for video monitoring. Biannual cross-shore elevation profiles at the study site are characterized by beach eroded shorelines and offshore sandbars in the winter, followed by accreted shorelines and onshore sandbars during low-energy summer wave conditions (Figure 2, Dingler & Reiss, 2002; Stevens et al., 2017).

The highest magnitudes of winter erosion at Sunset State Beach have occurred during El Niño periods, when storm tracks tend to shift southward in the Pacific Ocean and expose the northern Monterey Bay to larger waves (Storlazzi & Griggs, 2000). Dingler & Reiss (2002) surveyed cross-shore profiles at beaches throughout the Monterey Bay following a large El Niño event and observed that all surveyed beaches recovered on a similar timeline following the storm erosion. Their results suggest that sand was transported offshore during storms rather than alongshore. The previously observed interannual shoreline variability in Monterey Bay motivated additional tests of the shoreline change models on a longer time series of biannually surveyed shoreline positions, in addition to the video derived shoreline positions at Sunset State Beach.
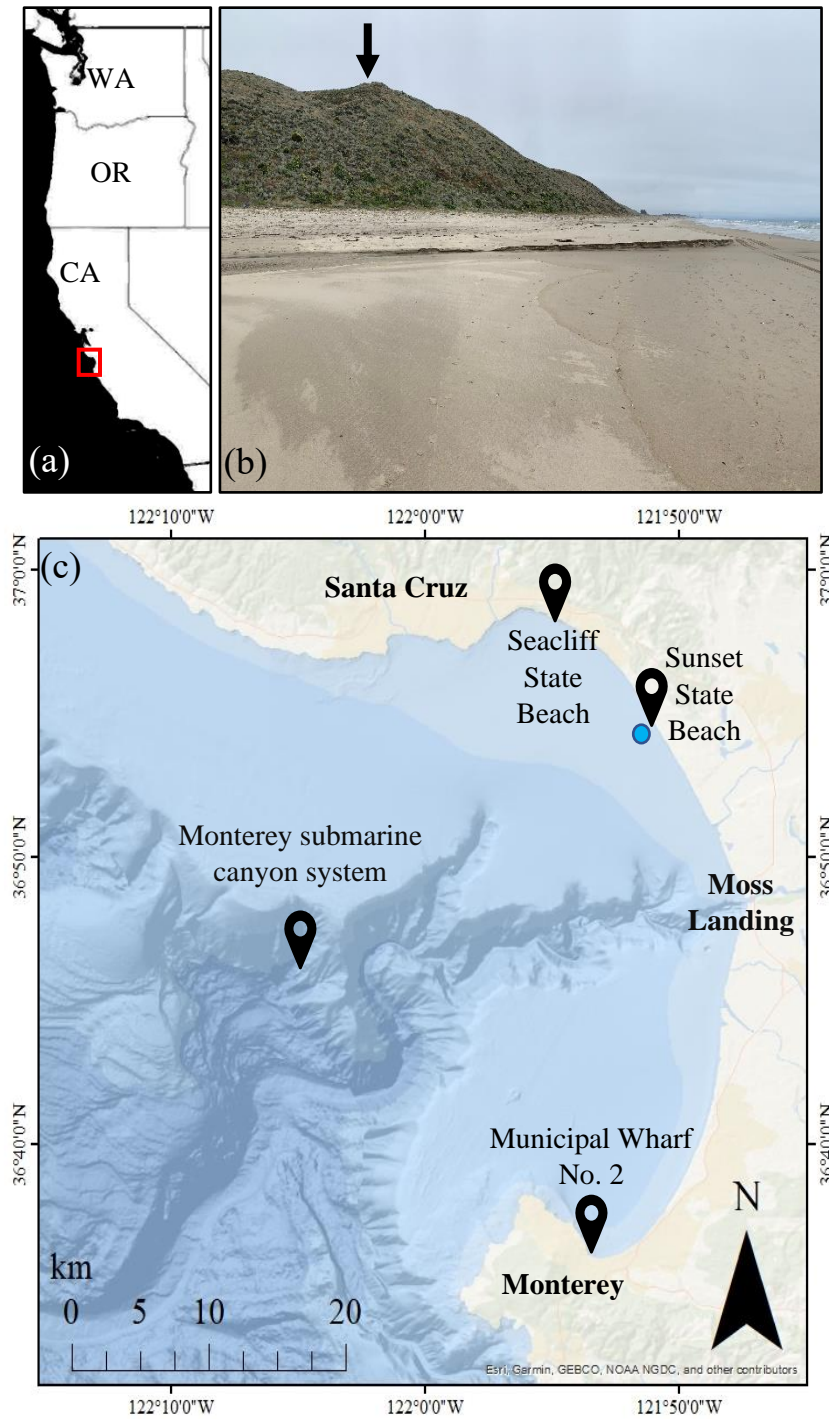
Figure 1: Map and characteristics of the study area. The Monterey submarine canyon system approaches shore in the Monterey Bay, located in central California (a). The video monitoring station is located atop the dune at Sunset State Beach, designated by the arrow in (b). The Monterey submarine canyon system refracts offshore wave energy as it approaches from the Pacific Ocean and enters the Monterey Bay (c). The blue point near Sunset State Beach represents the location of nearshore wave model estimates.
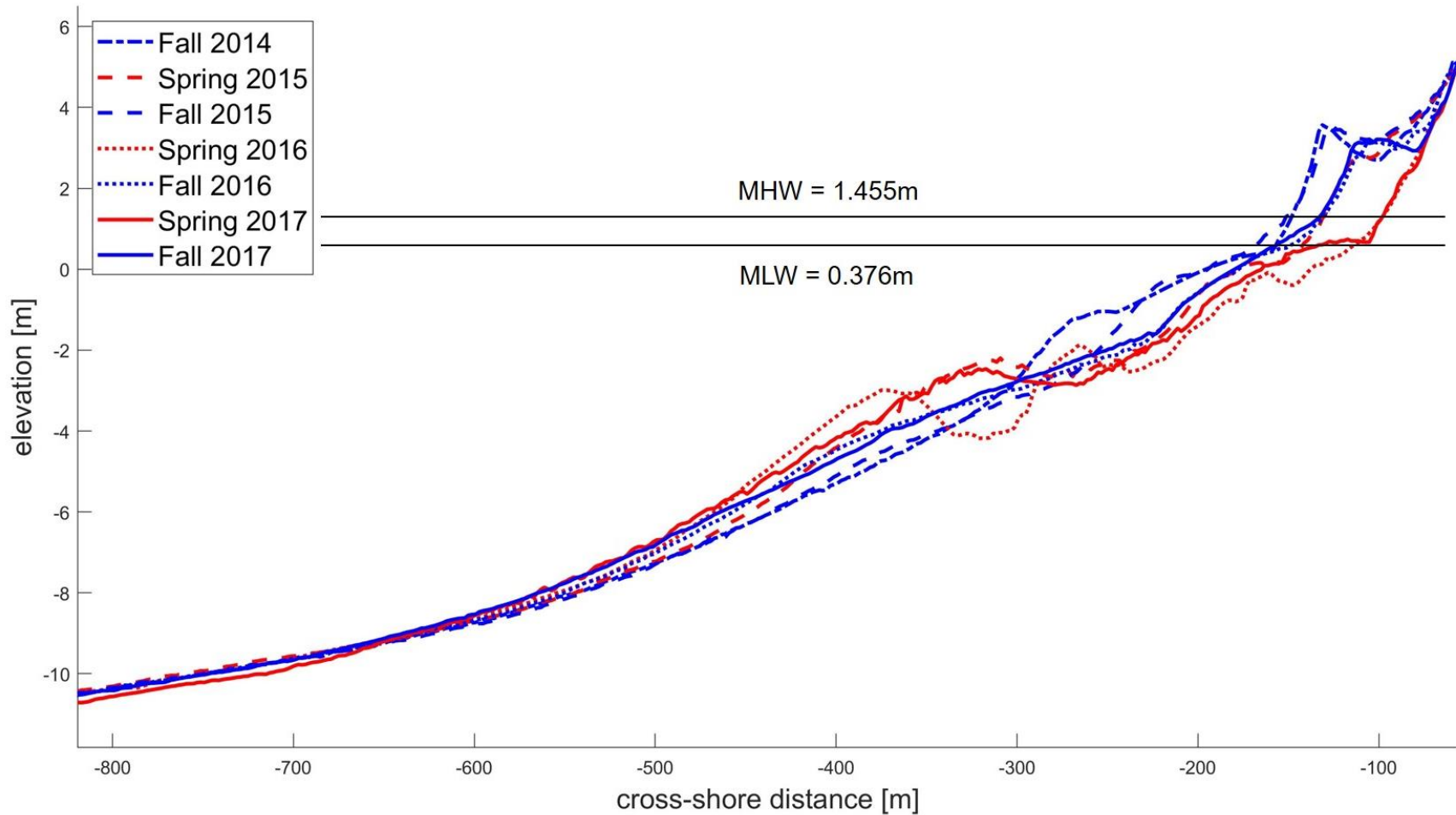
Figure 2: Biannual cross-shore beach profiles from Sunset State Beach. The intersect of the Mean High Water (MHW) tidal datum defined in Monterey and beach profiles define MHW shorelines. Mean Low Water (MLW) tidal datum with MHW indicates the typical tidal range at the study site. Elevation is referenced to NAVD88, where NAVD88 = 0m. Cross-shore distance is referenced to the dune base and is increasingly negative toward the west. All data was collected by USGS and is available online via Stevens et al. (2017).

SECTION 2

METHODS

The methods section is presented in three parts. First, the video monitoring station setup and methods applied to shoreline and sandbar mapping are described in Section 2a. Then, the nearshore wave model used in this study is summarized and validated in Section 2b. Finally, the shoreline model equations used to investigate the driving factors of shoreline change at the study site are described in Section 2c.

2a. Shoreline and Sandbar Mapping

A dual camera video monitoring station was installed in September 2017 at Sunset State Beach to continuously monitor coastal morphologic change (USGS 2017). Over the past 30+ years, video monitoring, also known as Argus monitoring, has become a useful method of measuring coastal hydro- and morphodynamic processes (Holman & Stanley, 2007). The Argus station used in this study was installed by the US Geological Survey (USGS) concurrent with their Fall 2017 nearshore bathymetry and beach topography survey campaign (Stevens et al., 2017). Shoreline and sandbar positions were mapped using time-exposure (timex) image products, made up of the average of all pixel values recorded at a 2Hz frame rate over 10 minutes, every half hour during daylight hours.

A combination of ground control points placed on the beach and extracted from personal watercraft tracks visible in "bright" image products were used to transform pixel coordinates in the oblique imagery to world coordinates. The bright image products contained only the brightest pixel values from the timex image products. Image products from both cameras were merged to create orthomosaics that were vertically rectified to distant tidal datum elevations. The orthomosaics were limited to a $600m^2$ domain to maintain consistent pixel resolution of 0.5m in both the along- and cross-shore directions throughout the study area (Figure 3). We use 20-months of imagery to build a time series of shoreline and sandbar positions at Sunset State Beach.

A local along- (**x**) and cross-shore (**y**) reference frame was defined to map shorelines and sandbars (Figure 3d). The vertical tolerances for image rectification are (**z** = Mean High Water (MHW) = 1.455m and **z** = Mean Low Water (MLW) = 0.376m) established at the National Oceanic and Atmospheric Administration (NOAA) tide gauge in Monterey (Station ID: 9412450), located approximately 30km south of Sunset State Beach. The tide gauge in Monterey is positioned outside of the surf zone at the end of the Monterey Municipal Wharf No. 2 (Figure 1c). The origin of the reference frame was defined as the **x** and **y** location of the camera system at MHW, 1.4m ≤ **z** ≤ 1.5m for shoreline mapping and MLW 0.3m ≤ **z** ≤ 0.4m for sandbar mapping. The vertical ranges around MHW and MLW used for image rectification were determined through trial and error to maximize the quantity of images that were captured near times when the water level approximated MHW and MLW. All vertical levels reported in this document were referenced to the North American Vertical Datum of 1988 (NAVD88).

Cross-shore shoreline positions were mapped using the color channel divergence (CCD) method, by subtracting the blue from red pixel values at cross-shore transects spaced every 5m alongshore (Figure 4a, Andriolo, 2019; Plant et al., 2007). The CCD method was implemented using the Shoreline-Mapping-Toolbox available on GitHub (Harley, 2019). Shoreline mapping at Sunset State Beach was successful on days when the water appeared bluer and failed on cloudy or foggy days when the water appeared greyer. Shorelines were only mapped when imagery coincided with MHW during daylight hours and was biased toward days when the water appeared bluer, resulting in an irregular time series of shoreline positions. Controlling shoreline mapping to MHW ensured that apparent shoreline migration from changes in water level was minimized (Moore et al., 2006). The CCD shoreline mapping method resulted in a cross-shore accuracy of ±5m for shoreline positions, on par with previous studies (i.e. Angnuureng et al., 2017; Senechal et al., 2015). However, additional error up to 12m or more was possibly induced from variations in nearshore wave setup, according to Angnuureng et al. (2017).

The cross-shore position of the outer sandbar, defined as the seaward-most high intensity band in timex products, was mapped manually at cross-shore transects spaced every 10 meters alongshore (Figure 4b). The seaward most band of high intensity pixels corresponded to the location of preferential wave breaking in the nearshore, acting as a proxy for the outer sandbar position (Lippman & Holman 1989). Sandbar mapping was limited to MLW to reduce any

apparent cross-shore migration due to changes in water level. For example, if we assume a constant sandbar position, waves of the same height would break farther offshore at low tide than at high tide. Mapping sandbar positions using timex products rectified to a low tide level allowed wave breaking to be most pronounced (van Enckevort & Ruessink, 2001).
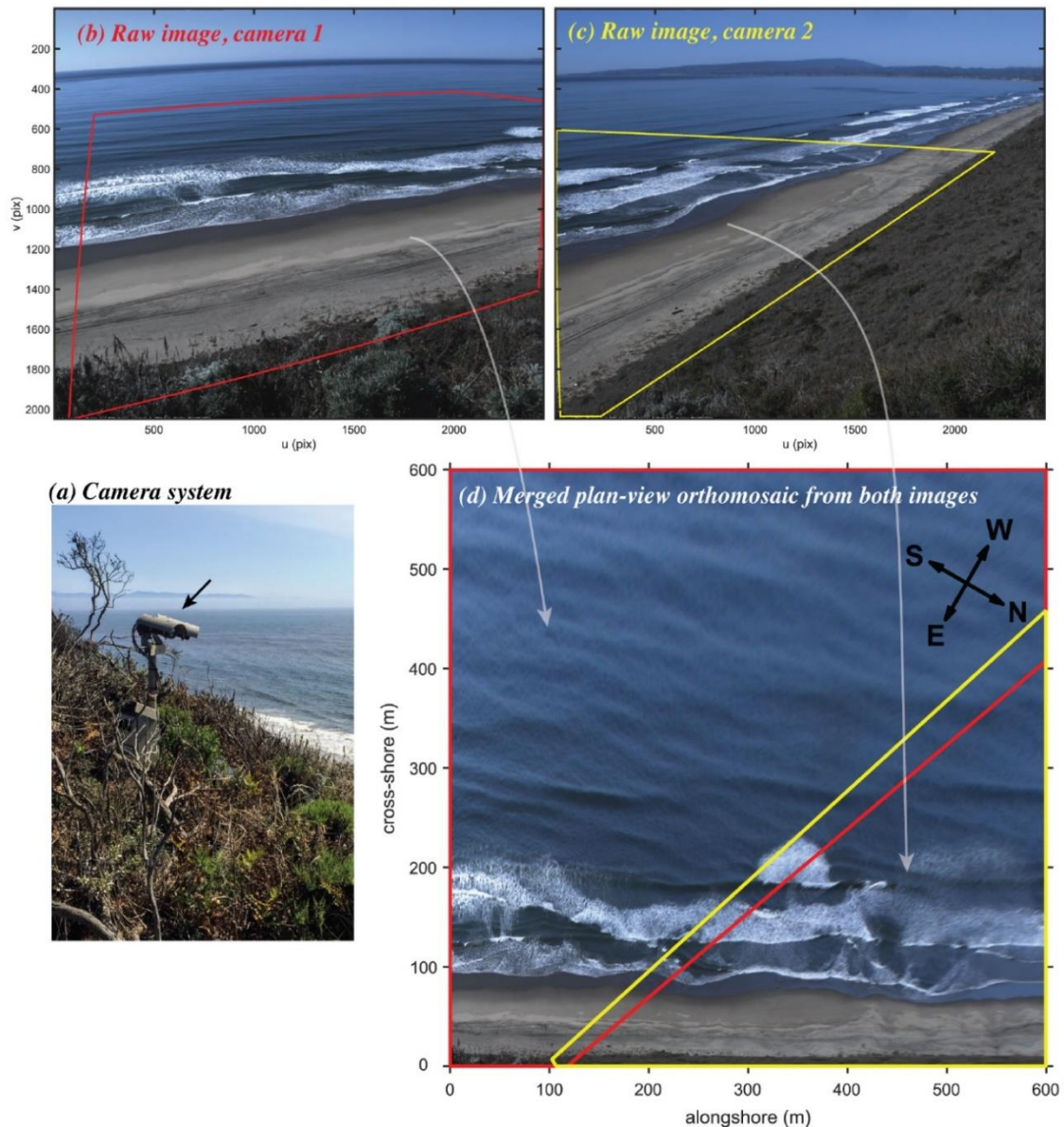
Figure 3: Dual camera Argus monitoring system at Sunset State Beach (a) and example of study area. Panels (b) & (c) show snapshots from camera 1 facing cross-shore and camera 2 facing alongshore. Axes in (b) & (c) are defined as image coordinates or pixel counts. An example of a rectified and merged orthomosaic (d) shows how each camera domain contributes to the study area that stretches 600m in the cross- and alongshore directions. Each pixel in (d) is 0.5 x 0.5m. Figure courtesy of Buscombe et al. (2020).

In addition to changing water level, previous studies have shown that image based proxy sandbar mapping is subject to uncertainties associated with changing wave height (Lippmann & Holman, 1990; van Enckevort & Ruessink, 2001). For example, larger waves may break further offshore at the seaward base of a sandbar, while smaller waves may break further landward at the crest of the sandbar. It is also possible that persistent foam at the preferred location of wave breaking may displace detection of the sandbar landward in high energy conditions, when the surf zone is saturated (Lippmann & Holman, 1990). In effort to reduce variations in sandbar position due to changing wave height, sandbar mapping was limited to times when nearshore significant wave heights were less than 1m. Sandbar mapping was further limited by times when waves were very small and it was unclear whether the sandbar was not visible in the imagery or was not present in the nearshore domain. An accuracy of ±10m was determined by visually interpreting the cross-shore range of possible outer bar positions that could have been mapped using this method, resulting in accuracy similar to previous studies such as Angnuureng et al. (2017) and Senechal et al., (2015).

The requirements applied to shoreline and sandbar mapping reduced cross-shore uncertainty but resulted in an irregular time series, sparse in comparison to the total number of image products collected between September 2017 to May 2019. If we consider an average of 8 hours of daylight per day with two timex products collected per hour, an approximate 10,000 timex products were collected during the study period at Sunset State Beach. By limiting shoreline mapping to MHW and sandbar mapping to MLW, the number of timex products used was greatly reduced (Tables 1 & 2). Sandbar mapping was further reduced by limiting wave conditions. A U.S. government shutdown prevented data collection in January 2019.

Previous observations of shoreline change in the Monterey Bay suggest annual variability in summer shoreline position, which motivated the investigation of a longer time series of shoreline positions at Sunset State Beach. MHW shoreline positions were extracted from the beach profiles surveyed by USGS (Figure 2). The latest publicly available data from USGS at the time of this study was from September 2017, so biannual shoreline positions were extracted from the video derived imagery to build a five-year time series of shoreline positions, from September 2014 to May 2019. The 5-year time series of biannual shoreline positions is used later, in the

shoreline modeling portion of this study to test the influence of cross- and alongshore sediment transport processes on shoreline change at Sunset State Beach.

Table 1: Quantity of shoreline extractions per month. 203 total timex products were mapped, but only 126 were used in shoreline modeling, shown in brackets. Grey boxes indicate months when shoreline mapping requirements were unmet, and no shorelines were mapped.

	Jan	Feb	Mar	Apr	May	Jun	Jul	Aug	Sep	Oct	Nov	Dec
2017	-	-	-	-	-	-	-	-	22 [12]	40 [20]	9 [7]	14 [10]
2018	4 [3]	7 [6]	13 [8]	6 [3]	0 [0]	1 [1]	8 [4]	20 [11]	10 [9]	19 [13]	9 [7]	11 [5]
2019	0 [0]	1 [1]	3 [2]	6 [4]	0 [0]	-	-	-	-	-	-	-

Table 2: Quantity of sandbar extractions per month. 80 total timex products were used. Grey boxes indicate months sandbar mapping requirements were unmet, and no sandbars were mapped.

	Jan	Feb	Mar	Apr	May	Jun	Jul	Aug	Sep	Oct	Nov	Dec
2017	-	-	-	-	-	-	-	-	-	6	8	6
2018	2	4	4	9	7	8	6	6	1	0	2	1
2019	0	0	2	5	3	-	-	-	-	-	-	-
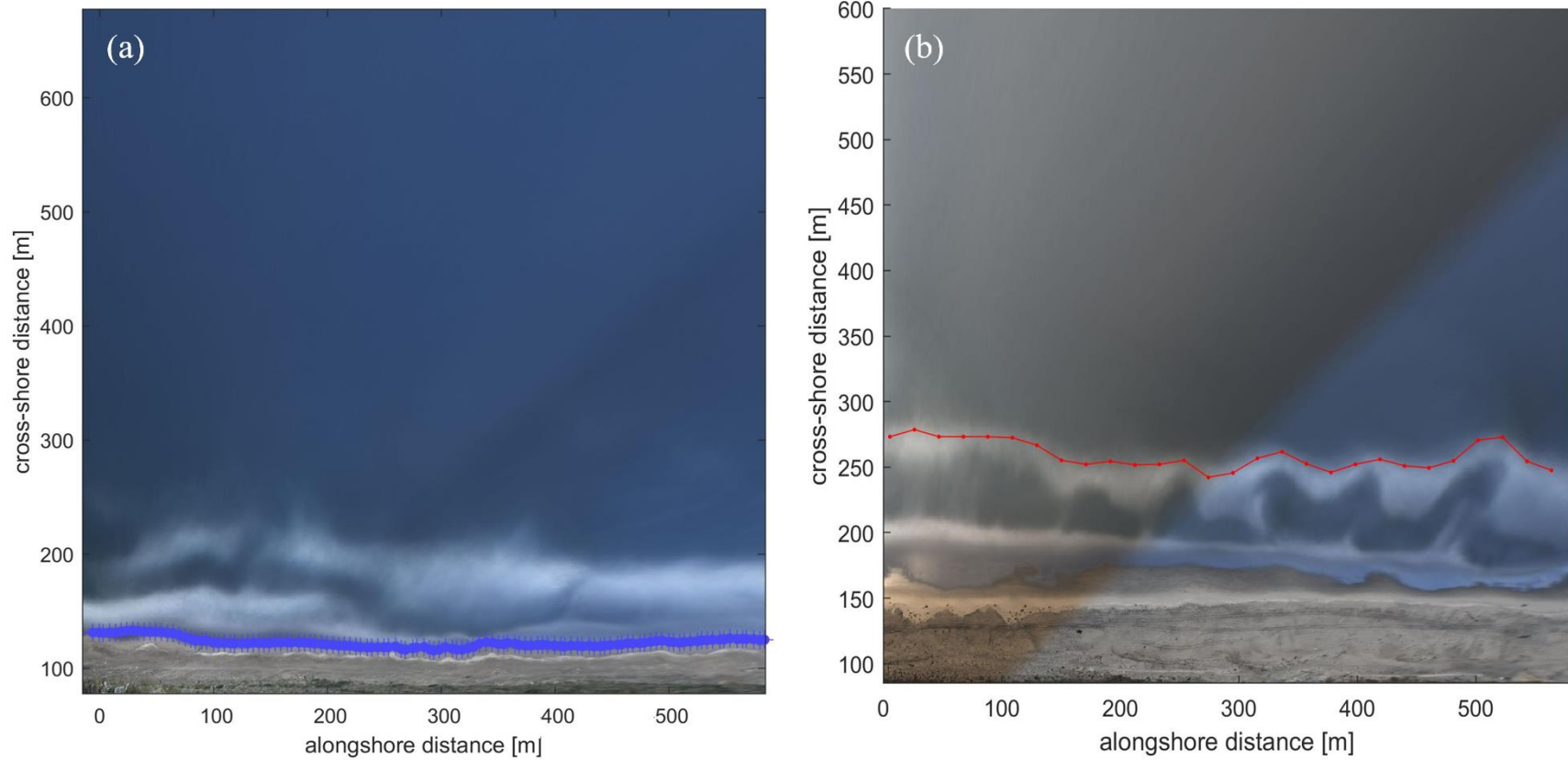
Figure 4: Example of shoreline (a) and sandbar (b) position mapping using rectified time exposure image products. The cross-shore shoreline position was mapped every 5 meters alongshore (cross hatches along blue line), while the cross-shore position of the outer sandbar was mapped every 10m alongshore (points along red line).

2b. Waves

The magnitude of wave energy and direction of wave approach were required to relate wave conditions to shoreline and sandbar positions, as well as force the shoreline change models used in this study. Modeled values of hourly nearshore wave statistics were gathered from the Coastal Data Information Program Monitoring and Prediction nearshore wave model for the 20-month study period (CDIP MOP). CDIP MOP produces wave estimates at 15m depth, spaced every 200m alongshore in central and northern California (O'Reilly et al., 2016). CDIP MOP uses offshore directional wave buoys to initialize the linear spectral wave propagation model including wave periods between 2-30 seconds, not including wave generation by local winds. To validate the CDIP MOP model near Sunset State Beach (CDIP MOP transect #SC024), USGS deployed a Nortek Acoustic Doppler Current Profiler (ADCP) for two months in the winter of 2017-18 collocated with the CDIP MOP model estimates. Between early December 2017 to the end of January 2018, nearshore significant wave height modeled by CDIP MOP ranged between 0.31m to 3.31m while waves measured by the ADCP ranged between 0.39m to 3.34m. During the two month ADCP deployment, in-situ wave characteristics closely matched with those predicted by CDIP MOP (RMSE = 0.13, r^2 = 0.91), justifying use for the duration of the study period (Figure 5). However, another ADCP deployment may be necessary to verify the utility of CDIP MOP nearshore wave predictions at other times of the year.
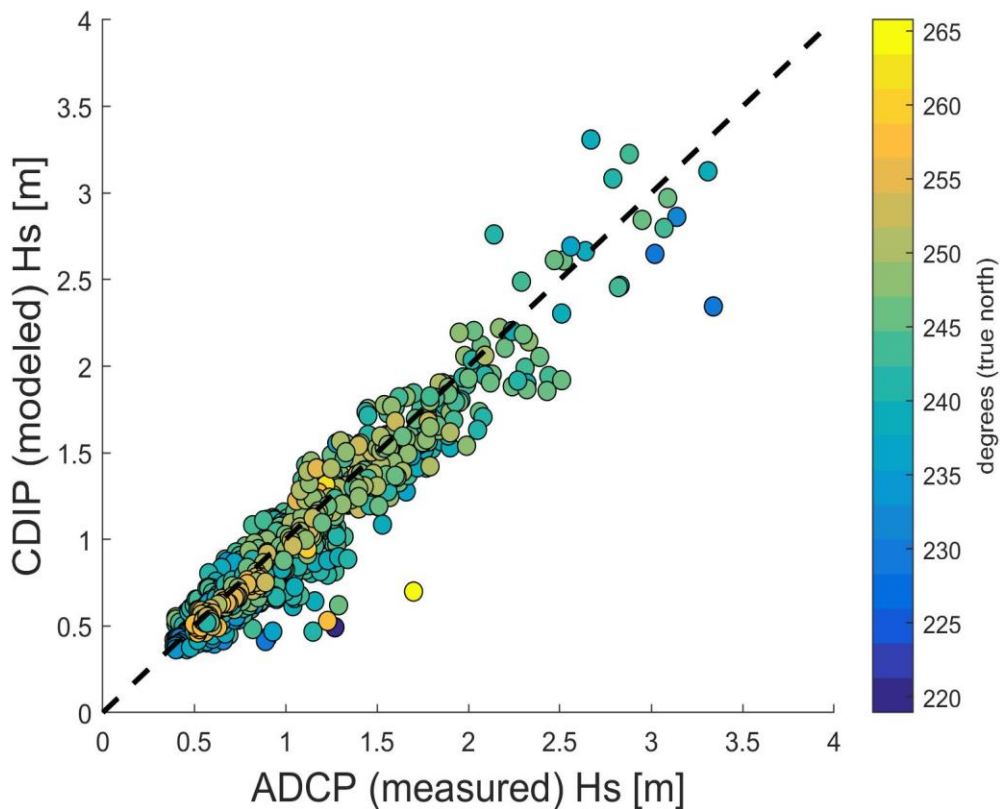
Figure 5: Modeled vs. measured nearshore significant wave height for December 2018 – January 2019. An Acoustic Doppler Current Profiler (ADCP) was co-located with CDIP MOP nearshore wave predictions in 15m depth offshore of Sunset State Beach. The gradual bathymetric slope from the inner shelf to the nearshore in Monterey Bay forces waves to have little variation from shore normal by the time they reach the nearshore. The points are colored by wave direction clockwise from true north, shore normal incident waves approach Sunset at 242˚ (green colored points). The linear slope is just less than 1 (dashed line) at 0.93m. ADCP data were collected and shared courtesy of Kurt Rosenberger of USGS.

2c. Shoreline Model Equations

Shoreline change due to cross- and alongshore sediment transport is estimated using simple shoreline change models, in three experiments. In the first experiment, shoreline change due to cross-shore sediment transport is estimated using a simple equilibrium shoreline change model, assuming shore-normal incident waves (Yates et al., 2009). In the second experiment, shoreline change due to alongshore sediment transport is tested using the Coastal Engineering and Research Center (CERC) equation (USACE, 1984). In the final model experiment, the equilibrium and CERC models are combined to test the overall influence of wave energy and

wave direction to the observed shoreline change at Sunset State Beach. In general, the modeling workflow consisted of estimating initial model parameters from previous studies, optimizing the model parameters to Sunset State Beach, and testing the model skill against shoreline observations.

According to the equilibrium shoreline change model proposed by Yates et al. (2009), shoreline change over time $\frac{dS}{dt}$ in $[\frac{m}{day}$ or $\frac{m}{hour}]$,

(1) $\frac{dS}{dt} = C^{\pm} \sqrt{E}$ (ΔE)

depends on the energy-shoreline disequilibrium ΔE $[m^2]$, where

(2) $\Delta E = E - E_{eq}(S)$.

When $\Delta E = 0$, the shoreline is assumed to be in equilibrium with wave energy, so theoretically, no shoreline change would occur if a constant wave energy persisted. The energy-shoreline disequilibrium is defined as the difference between the current wave energy E and estimated wave energy equilibrium E_{eq}, which is a linear function of shoreline position, S $[m]$, where

(3) $E_{eq}(S) = aS + b$.

The equilibrium shoreline change model has four free parameters: an erosion/accretion coefficient $C^{\pm}$ [energy$^{-2} \cdot$ time^{-1} in $m^{-2} \cdot hr^{-1}$], a linear slope a [$\frac{\text{wave energy}}{\text{meter}}$ in $\frac{m^2}{m}$], and y-intercept b [wave energy in m^2]. The accretion parameter C^{+} is used when $\Delta E < 0$ and accretion is required for the shoreline to reach equilibrium, while the erosion parameter C^{-} is used when $\Delta E > 0$ and erosion is required for the shoreline to reach equilibrium with wave conditions. The parameters a and b define the linear relationship between the shoreline position and equilibrium wave energy. Equation (3) estimates the observed average wave energy that caused no shoreline change during the study period. The e-folding scale ($[aC^{\pm}E^{\frac{1}{2}}]^{-1}$) where $(E = \frac{H_s^2}{16})$, or the time to shoreline adjustment, is inversely proportional to significant wave height and can be used to calculate the theoretical timescales of shoreline erosion and accretion.

For consistency with previous studies by Yates et al. (2009, 2011), the temporal mean from the time series of shoreline positions was removed. Additionally, nearshore significant wave height Hs $[m]$ was converted to a proxy for nearshore wave energy E $[m^2]$ to enable parameter comparisons with Yates et al. (2009, 2011), where

(4) $E = \frac{1}{16}Hs^2.$

In the first model experiment, the equilibrium shoreline change model was tested using the 20-month time series of video derived shorelines and the biannual time series of USGS surveyed shorelines at Sunset State Beach. Initial estimates of equilibrium model parameters a and b were calculated using a linear fit between observed S and the averaged wave energy between shoreline position observations, S, following Yates et al. (2009). The number of shoreline observations used in shoreline modeling was reduced in this step to one observation per day to reduce noise in shoreline change rate calculations within shoreline mapping uncertainty (Table 1). $C^{\pm}$ was estimated by solving equations (1), (2), and (3) using shoreline change calculations from observations and the initial estimates of a and b. However, the initial parameter estimates resulted in unreasonable shoreline predictions. The time between observed S ranged from 1 to 57 days, which smoothed wave energy between shoreline observations significantly, thereby deeming this method of initial parameter estimation ineffective. Therefore, model parameters calculated by Yates et al. (2009, 2011) were enlisted as initial parameter estimates at Sunset State Beach.

Yates et al. (2009) calculated model parameters for a beach in southern California with lower wave energy and Yates et al. (2011) calculated model parameters for a beach in northern California with higher wave energy compared to Sunset State Beach. Therefore, the model parameters a and $C^{\pm}$ calculated by Yates et al. (2009, 2011) were averaged under the hypothesis that the averaged parameters would provide accurate predictions of shoreline change at Sunset State Beach. The site-specific parameters b and the initial shoreline position (S_0) were determined specifically for Sunset State Beach, since they relate around the temporal mean and is different from site to site.

Using the averaged Yates et al. (2009, 2011) model parameters, parameter optimization procedures were used to improve hourly model estimates of shoreline position by adjusting model parameters to yield the best overall fit between model predictions and shoreline observations. Each parameter and S_0 were optimized using a simulated annealing (SA) framework to find the best combination of parameters. SA works by minimizing a cost function between model predictions and observations and finds the global minimum within the four-dimensional parameter space (Glover, Jenkins, & Doney, 2011). All parameter optimization procedures were implemented using the MATLAB Optimization Toolbox.

In the second model experiment, the CERC equation was used to test the influence of wave direction in addition to wave energy at the study site (USACE 1984). Shoreline change due to alongshore sediment transport $(\frac{dS}{dt})$ was then calculated using a finite difference between sediment transport volumes 400m north and 400m south of Sunset State Beach $(\frac{dQ}{dy})$ at CDIP MOP transects SC026 and SC022, where

(5) $\quad \frac{dS}{dt} = \frac{1}{H_{cl}} \frac{dQ}{dy}.$

The depth of closure (H_{cl}), defined as the seaward limit of sediment transport, was set to 10m. The alongshore sediment transport volume, Q, is a function of time and alongshore distance which depends on one free parameter K, alongshore radiation stress (S_{xy}), and phase velocity at breaking (C_p) (Crosby et al., 2016).

(6) $\quad Q = K \, S_{xy} \, C_p$

The initial estimate for K was set at 0.6 following the results of Crosby et al., 2016 and S_{xy} values were acquired from CDIP MOP. The depth at which waves were breaking was estimated at approximately 1.3 times the significant wave height, yielding similar estimates of breaker depths to those calculated by Camenen & Larson, 2007. C_p was calculated assuming intermediate waves. Parameter optimization was conducted for all parameters except H_{cl}, using SA, described previously. The parameter H_{cl} is inversely related to the parameter K so was not expected to alter the shoreline model results since K was optimized.

In the final model experiment, the equilibrium model and CERC equation, (1) and (5), were combined to test the influence of wave energy and wave direction to the observed shoreline change at Sunset State Beach, where overall shoreline change over time is

(7) $\quad \dfrac{dS}{dt} = C^{\pm} \sqrt{E}\ (\Delta E)\ +\ \dfrac{1}{H_{cl}} \dfrac{dQ}{dy}.$

The combined model was tested on the 20-month time series of video derived observations as well as a biannual time series of shoreline positions to quantify the overall contribution cross- and alongshore sediment transport to observed shoreline change at Sunset State Beach.

SECTION 3

RESULTS

The results section is presented in two parts. First, the relationships between shoreline, sandbar, and nearshore waves are described in Section 3a. Second, the results of the three modeling experiments are shown in Section 3b.

3a. Shoreline, Sandbar, and Waves

The relationships between shoreline and sandbar positions with wave conditions were quantified to investigate the ability of the sandbar to buffer the shoreline and delay winter shoreline erosion. Shoreline and sandbar positions were mapped within a 600m alongshore stretch of beach. Alongshore shoreline and sandbar variability were defined by the standard deviation of each shoreline or sandbar position within the 600m study area.

Alongshore shoreline variability ranged between 2m to 8m throughout the study period, with a median variability of 4m (Figure 6) From September to December 2017, the shoreline eroded by a total of about 32m and accreted by a total of 45m from December 2017 to June 2018. From late August to early December of 2017, the shoreline remained relatively stable but slowly eroded by approximately 10m during these 3 months. Larger wave events in mid-late December corresponded with 22m of shoreline erosion over the course of 2-3 weeks. By late January the shoreline accreted by 15m and continued to accrete through the spring until June 2018, when the shoreline reached a stable position 10m seaward of the stable shoreline position in the previous year. The shoreline remained stable in the summer of 2018 until the onset of large wave events drove approximately 58m of erosion during the winter of 2018-2019. With sustained high wave energy in winter of 2018-2019, the shoreline remained eroded into March 2019 and began to accrete under lower energy conditions in mid-late March 2019. The shoreline remained stable from June to early November 2018, then eroded further to a total of about 55m by February 2019. Significant shoreline erosion was only observed when waves exceeded the 95th percentile, 1.7m (Figure 6).

Compared to the shoreline, the sandbar at Sunset State Beach had a greater cross-shore range in position and alongshore variability (Figure 6). Alongshore sandbar variability ranged

between 2m to 23m, with a median variability of 7m. Increased sandbar variability generally corresponded to 3D morphologies where rip channels and cuspate sandbar formations were apparent in the timex products. From September 2017 to late March 2018 the sandbar gradually migrated 100m seaward during the 6-month period. This migration then reversed direction and the sandbar migrated 100m landward over the following 5 months, until early August 2018. By November 2018, the sandbar migrated seaward nearly as far as in the previous year, however very few sandbar positions were extracted from the imagery during the winter of 2018 – 2019. By March 2019 the alongshore variability of the sandbar reached its maximum and the sandbar remained at a variable seaward position until the end of the study period.

The sandbar generally migrated offshore as wave energy increased and onshore as wave energy decreased. Sandbar positions correlated more strongly with wave heights ($r^2 = 0.40$) better than shoreline positions ($r^2 = 0.25$) (Figure 7). This pattern is more apparent in 2017-2018 (referred to as year 1) than 2018-2019 (year 2) due to the greater quantity of observations (Figure 7). The sandbar was farthest seaward in the spring of both years (green points) and the farthest landward in the fall (blue and purple points).

Sandbar positions were only extracted from imagery when CDIP MOP significant wave height was reported at less than 1m (Figure 7). Since waves tend to break at distinct depths (smaller waves in shallower water and larger waves in deeper water), the approximate elevation at wave breaking was calculated when sandbar positions were mapped to confirm that observed sandbar migration was not an artifact of waves breaking at various depths. The beach slope at Sunset State Beach was approximately 0.03 based on survey data in fall 2017 (Figure 2) and the elevation where waves were expected to break ranged by 0.93m (calculated following Camenen & Larson (2007)). The expected depth at wave breaking corresponded to a 27m cross-shore range, while the observed range of sandbar migration was approximately 100m during the study period. According to the survey data the cross-shore profile at Sunset State Beach became steeper in winter months, which reduced the cross-shore range of wave breaking. Since the observed range in sandbar position was an order of magnitude greater than the cross-shore range of depth where waves were expected to break, it is unlikely that requirements applied to sandbar mapping influenced the observed range of migration significantly.

Shoreline and sandbar positions were inversely correlated; the sandbar migrated seaward while the shoreline eroded under high energy conditions and vice versa, with certain exceptions (Figure 8). The relationship was mainly driven by seasonal changes in wave energy but was weaker than expected due to differences in the timing of sandbar and shoreline migration. For example, the sandbar migrated offshore consistently from September 2017 to April 2018 before reversing direction, while the shoreline remained static until the first wave event exceeding 1.7m in December 2017. In late September 2017 and early November 2017, the significant wave height did exceed 1.7, but did not affect the shoreline position since the events were very short. Before the first large wave event in year 1 (Figure 8, points 2-5) and year 2 (Figure 8, points 12-15), the shoreline position remained relatively stable while the sandbar migrated offshore, deviating from the linear relationship. After the first large wave event when the shoreline had eroded in each year (Figure 8, points 6-10 for year 1 & points 17-23 for year 2), the sandbar continued migrating offshore, while the shoreline accreted much more rapidly in year 1 than in year 2.
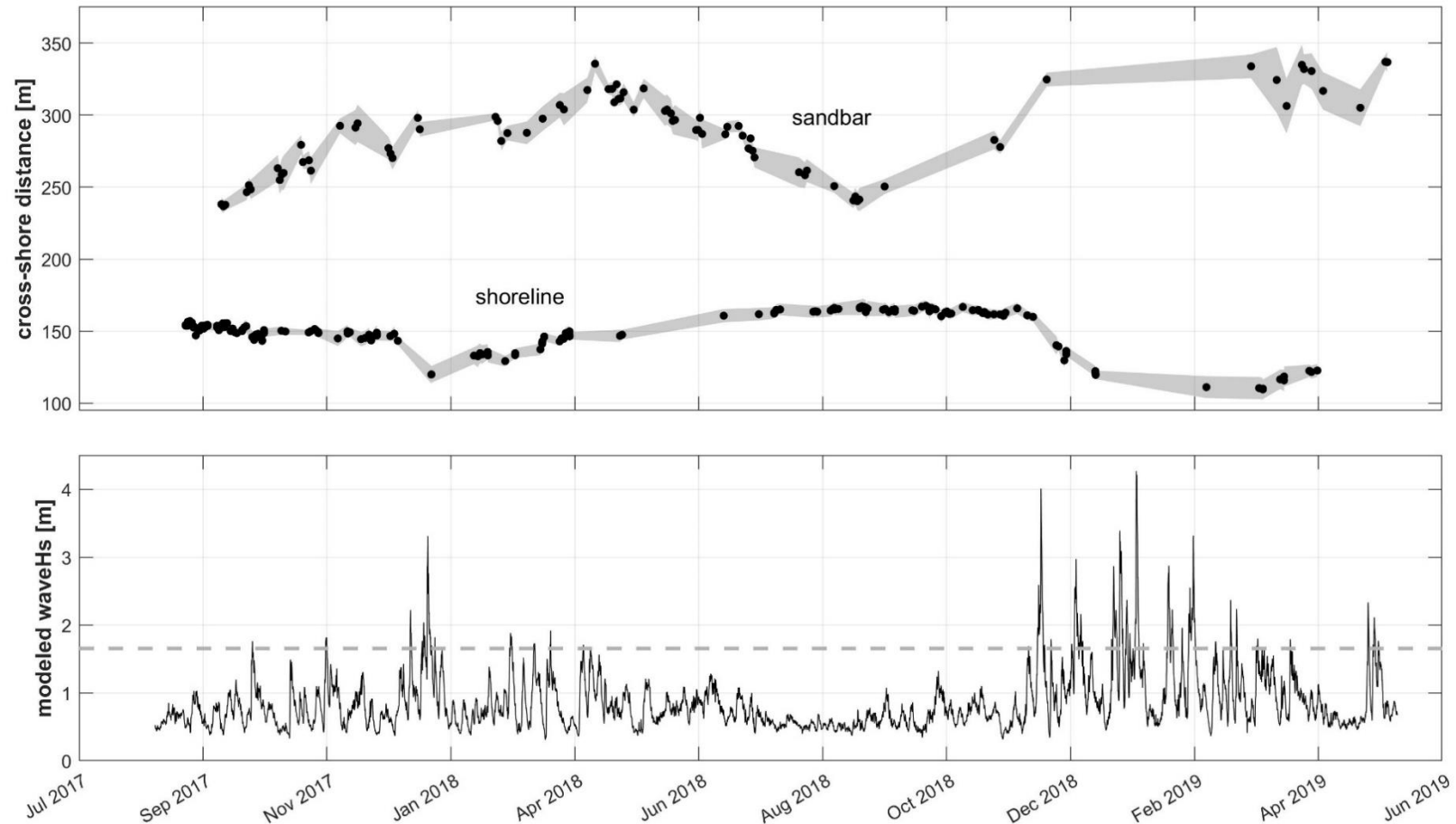
Figure 6: Time series of all imagery mapped shoreline and sandbar positions. In the top panel, the black points represent the alongshore averaged sandbar or shoreline position mapped from imagery and the grey envelope indicates the alongshore variability, or standard deviation of the 600m stretch of sandbar or shoreline. The envelope is interpolated between observations so does not necessarily represent observed change. The bottom panel shows CDIP MOP nearshore significant wave height near Sunset State Beach and the dotted line suggests a wave energy - shoreline erosion threshold at the 95th percentile, 1.7m at Sunset State Beach.
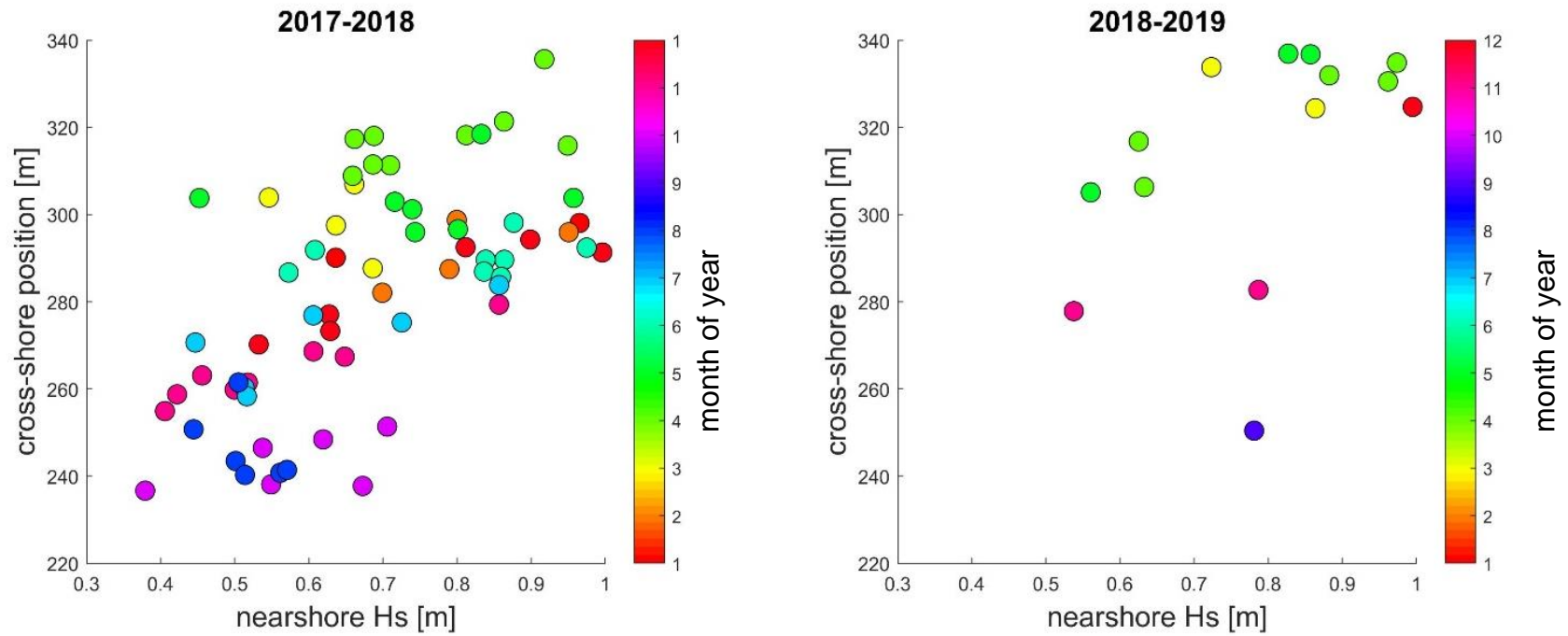
Figure 7: Cross-shore sandbar position vs. nearshore significant wave height (Hs) for year 1: October 2017 – August 2018 (left) and year 2: September 2018 – April 2019 (right). Data is colored by month of year (January = 1, February = 2, etc.). Sandbar position was positively correlated with wave height, the overall $r^2 = 0.40$ for all sandbar observations.
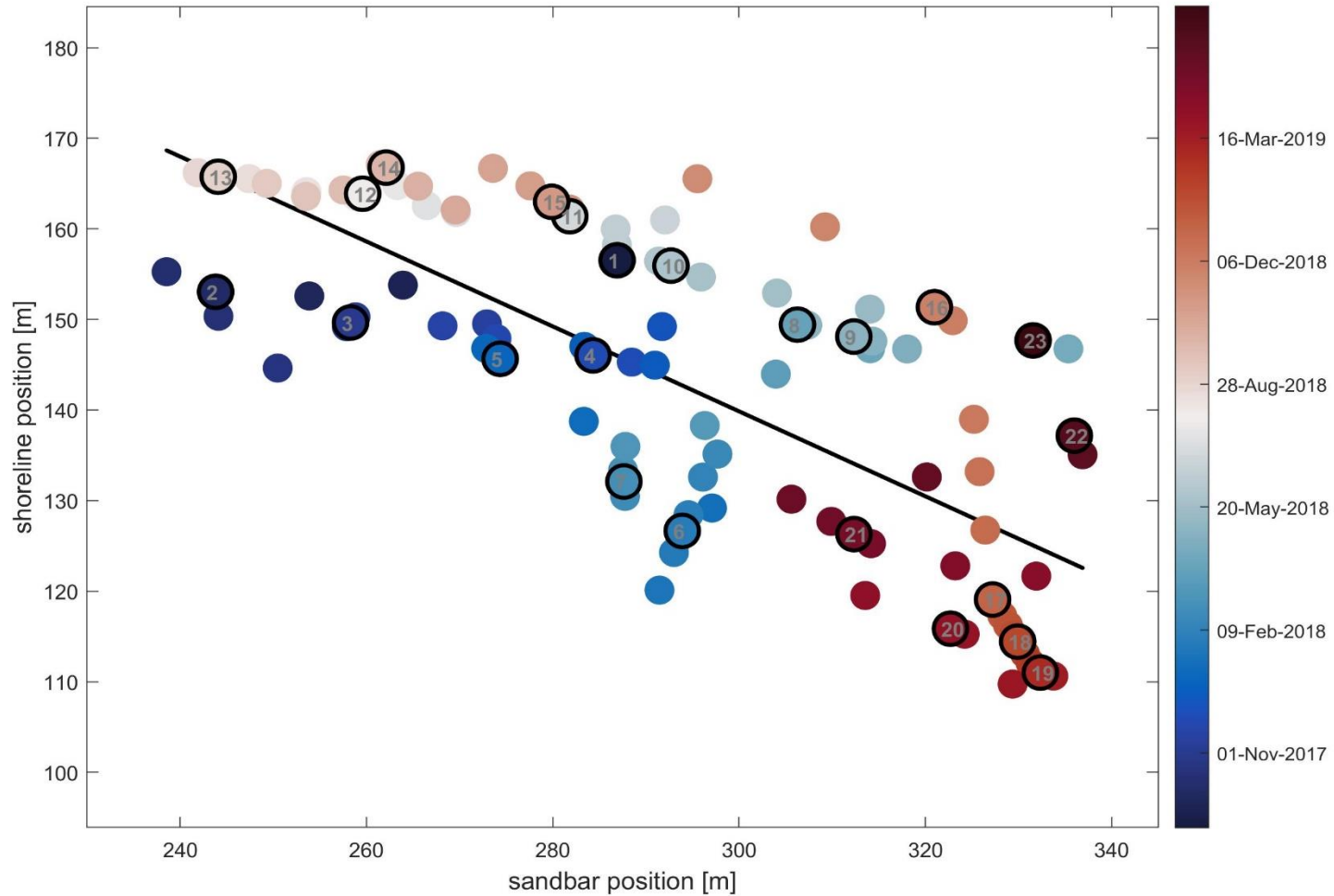
Figure 8: Weekly shoreline vs. sandbar positions at Sunset State Beach colored, r2 = 0.57 and linear slope is -0.47m (black line). Since shoreline and sandbar positions were not observed at the same time during the study period, the time series were synchronized and interpolated to display weekly observations and are colored by time. Monthly positions are outlined in black and numbered beginning at 1 in October 2017 (darkest blue).

According to the video derived shoreline positions, the seasonal pattern at Sunset State Beach was generally described by rapid shoreline erosion with high energy waves and gradual accretion with low energy waves. Shoreline erosion and accretion depended on both wave energy and the previous shoreline position, suggesting an equilibrium shoreline response (Figure 9). Accreted shorelines exposed to high energy conditions were generally observed to erode (red points in Figure 9) and eroded shorelines exposed to low energy conditions were observed to accrete (blue points in Figure 9). There were some exceptions in the time series (where blue points fell above the equilibrium state (black line in Figure 9), or red points fell below), but the seasonal equilibrium response dominated the observed shoreline change patterns.
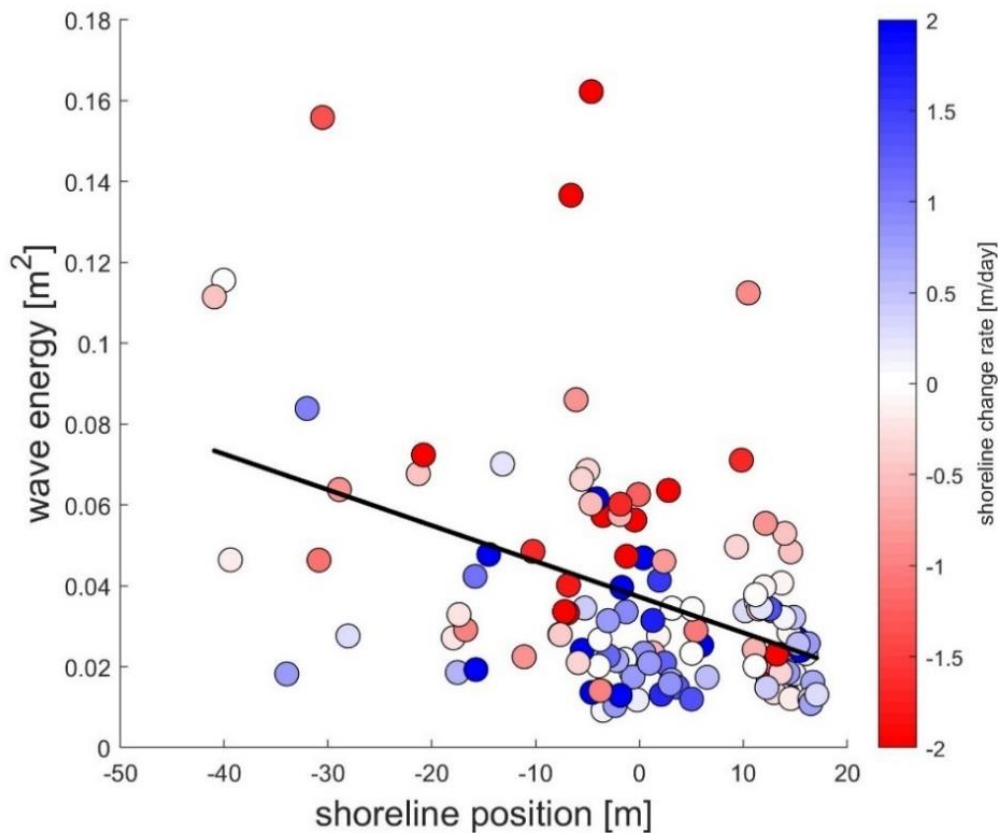
Figure 9: Shoreline change rate $\frac{dS}{dt}$ between consecutive shoreline observations and averaged wave energy at Sunset State Beach. The black line shows the linear fit ($r^2 = 0.25$) used to determine initial parameters (y-intercept $b = 0.037m$, slope $a = -0.00081\ m^2/m$). The black line represents an estimated equilibrium state where no shoreline change is expected according to shoreline position and wave energy.

3b. Shoreline Modeling

Three model experiments were conducted to test the contribution of cross- and alongshore sediment transport processes to observed shoreline change at Sunset State Beach. In the first model experiment, an equilibrium shoreline change model was used to test the influence of cross-shore sediment transport to shoreline change at Sunset State Beach. In the second model experiment, the CERC equation was used to test the influence of alongshore sediment transport to shoreline change at the study site. In the third model experiment, the equilibrium shoreline change and CERC models were combined to test the contribution of wave energy and wave direction to observed shoreline change at Sunset State Beach. Each experiment was conducted to test the drivers of shoreline change at the study site, which is sheltered by headlands and fronted by a submarine canyon system with irregular bathymetry.

In the first model experiment, a simple equilibrium shoreline change model was tested to quantify the influence of shore-normal incident wave energy to shoreline change with 20 months of video derived observations. Shoreline predictions using the averaged parameters from Yates et al. (2009, 2011) predicted shoreline change with a root mean squared error (RMSE) of 8.0m (Table 3). For comparison, the model parameters calculated at Ocean Beach and ran directly at Sunset State Beach resulted in an RMSE of 9.1m and those calculated at Torrey Pines resulted in an RMSE of 7.9m (Table 3). After optimizing the equilibrium model parameters at Sunset State Beach, the equilibrium shoreline model reaches an RMSE of 6.4m. For comparison, the optimized RMSE values for both Ocean Beach and Torrey Pines approximate 5m (Yates et al. 2009, 2011). The optimized equilibrium model (grey line in Figure 10) shows rapid erosion at the onset of winter in both years, consistent with observations. The shoreline position is overestimated in the fall of 2017 but underestimated in the fall of 2018. The shoreline erosion observed in the winter of 2017-18 is underestimated, while the shoreline erosion in the winter of 2018-19 is better represented by the equilibrium model.

Table 3: Shoreline modeling parameters, associated sensitivity, and model skill for each model experiment using 20 months of video derived shoreline positions. Grey rows indicate parameters calculated by Yates et al. (2009, 2011) and the green rows show parameters optimized at Sunset State Beach. The parameter *b* and the initial shoreline position from the optimized equilibrium model parameters (Eq) was used to run the Ocean Beach, Torrey Pines, and Averaged parameters at Sunset. RMSE is reported for the model runs between fall 2017 and spring 2019, according to imagery mapped shorelines. Parameter sensitivity is defined as the range of parameter values where the RMSE varied less than 10%, calculated for optimized parameters.

	a $[10^3\ m^2/m]$	b $[m^2]$	C^- $[m^{-2} \cdot hr^{-1}]$	C^+ $[m^{-2} \cdot hr^{-1}]$	S_0 $[m]$	K	RMSE $[m]$
Initial Estimate	-0.81	0.037	-17.72	-28.047	5.45	-	27.3
Ocean Beach	-3.6	0.064	-0.54	-0.83	0.012	-	9.1
Torrey Pines	-4.5	0.064	-1.38	-1.16	0.012	-	7.9
Averaged	-4.0	0.064	-0.96	-1.00	0.012	-	8.0
Optimized (Eq)	**-2.2** ± 1	**0.064** ± 0.5	**-1.02** ± 0.5	**-1.02** ± 0.5	$-14.60 \leq$ **0.0020** ≤ 4.02	-	6.4
Optimized (Eq & CERC)	**-2.8** ± 1	**0.081** ± 0.5	**-1.05** ± 0.5	**-1.04** ± 0.5	$-10.12 \leq$ **0.048** ≤ 3.61	**0.61** ± 0.3	5.6
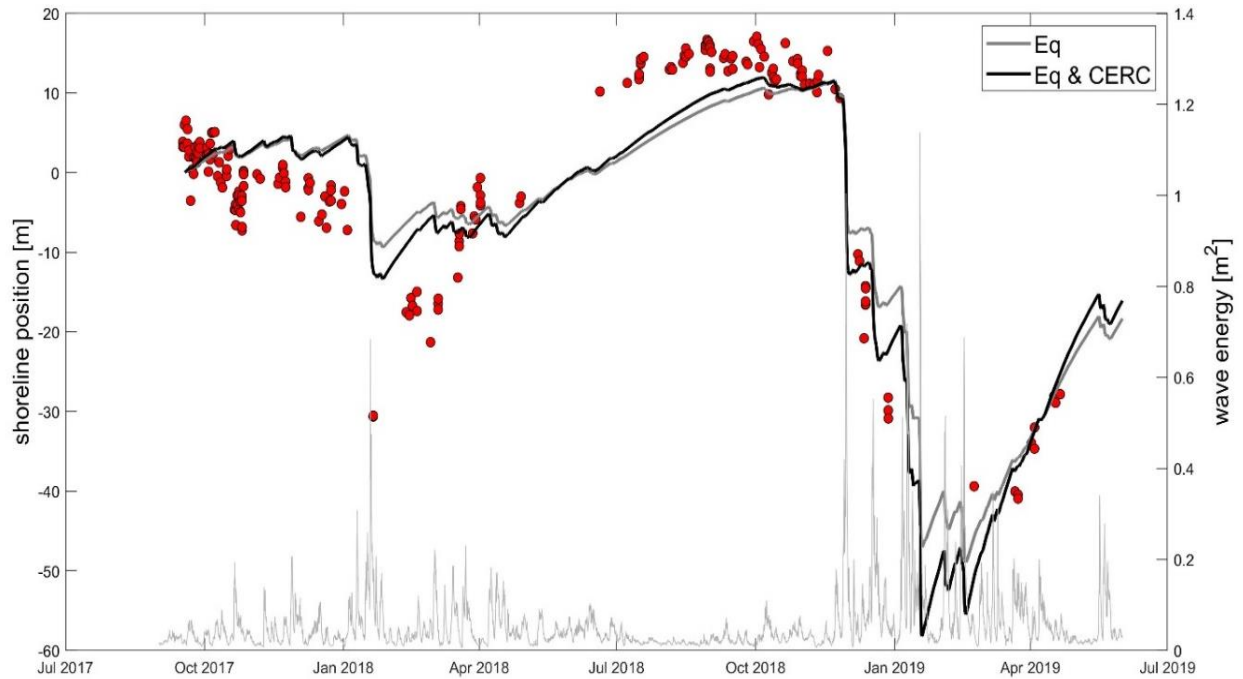
Figure 10: Equilibrium shoreline model predictions using optimized parameters for image mapped shorelines from fall 2017 to spring 2019. Hourly model predictions are shown in black for the Equilibrium model expanded with CERC and grey for the equilibrium model alone. Shorelines mapped by imagery are shown by red points. Wave energy is shown in light grey according to the right axis.

The optimized parameters a, $C^{\pm}$, and typical significant wave heights for erosion and accretion events at Ocean Beach, Torrey Pines, and Sunset State Beach were used to compute the timescales of erosion and accretion. The e-folding scale ($[aC^{\pm}E^{\frac{1}{2}}]^{-1}$) where ($E = \frac{H_s^2}{16}$), or the time to shoreline adjustment, is inversely proportional to significant wave height. Following Yates et al. (2011), theoretical wave events of $H_s = 1m$ and $H_s = 4m$ were considered to represent accretional and erosional shoreline adjustment to maintain comparability between sites (Table 4). If $H_s = 4m$ wave conditions were sustained, it would take Sunset State Beach 19 days, just under three weeks, to erode to an equilibrium shoreline position. On the other hand, if $H_s = 1m$ conditions were sustained, it would take Sunset State Beach 74 days, just over two months, to accrete to an equilibrium shoreline position.

Table 4: Erosion and accretion timescales. Ocean Beach and Torrey Pines values were calculated by Yates et al. (2011) and the ± values represent alongshore averages over approximately 7km of beach. Timescales at Sunset State Beach were determined in the present study for alongshore averaged shorelines along 600m of beach, so ± values are not reported.

	Erosion Timescale (days)	**Accretion Timescale (days)**
Ocean Beach	43 ± 39	107 ± 66
Torrey Pines	9 ± 4	52 ± 29
Sunset State Beach	19	74

According to observations, the shoreline was in an erosional state for approximately 18 days and an accretional state for approximately 219 days in year 1. A wave event exceeding 1.7m (95th percentile) occurred on January 10, 2018 but only lasted 12 hours. About 8 days later, another wave event exceeding 1.7m lasted for about 2 days. Compared to the 74-day accretion timescale, the time between wave events was only 8 days in year 1 and the shoreline was unable to recover prior to the second large wave event. In year 2, the shoreline was in an erosional state for 125 days and appeared to actively be accreting at the end of the study period. Wave events exceeding 1.7m occurred beginning in late November 2018 and tended to reoccur every three weeks until early March of 2019. Since the time between wave events was much less than the accretion timescale, the shoreline was unable to accrete during the prolonged stormy period. The shoreline was able to begin accreting much sooner with the shorter duration of wave events exceeding 1.7m in year 1, compared to the longer duration in year 2.

In the second model experiment, shoreline change due to alongshore sediment transport was computed using the CERC equation to investigate the influence of wave direction to overall shoreline change at Sunset State Beach. The direction and magnitude of sediment transport is proportional to the alongshore radiation stress (equation 6), where positive values indicate northward sediment transport and negative values indicate southward sediment transport (Figure 11a). Shoreline change occurs when the alongshore radiation stress diverges alongshore, causing a loss or gain of sediment from a discrete point on the beach. This happened for example, in

winter 2, when the alongshore radiation stress drove northward sediment transport to the north of Sunset State Beach and southward sediment transport to the south (Figure 11a).

The maximum sediment transport divergence in winter 2 corresponds to the highest estimated rate of cumulative shoreline change due to alongshore sediment transport during the 20-month study period (Figure 12b). The cumulative shoreline change shows the amount of expected shoreline change over time due to the alongshore sediment transport gradient. During the 20-month study period, approximately 40m of shoreline erosion was attributed to alongshore sediment transport processes (Figure 12b). According to the cumulative shoreline change calculation due to alongshore sediment transport processes, no shoreline accretion occurred during the study period.

The magnitude of shoreline erosion due to alongshore sediment transport processes increased when offshore waves approached from the west. Waves measured at an offshore buoy approached from the northwest in year 1 (Figure 12c), while offshore waves approached from the west in year 2 (Figure 12d). A lower magnitude of shoreline erosion occurred due to alongshore sediment transport in winter 1, likely because wave conditions measured at the offshore buoy approached from the northwest and Sunset State Beach was better protected from incoming waves by the Santa Cruz headlands. Greater alongshore sediment transport divergence occurred as waves approached the shoreline in winter of year 2, possibly contributing to a greater magnitude of winter shoreline erosion than in the previous year.
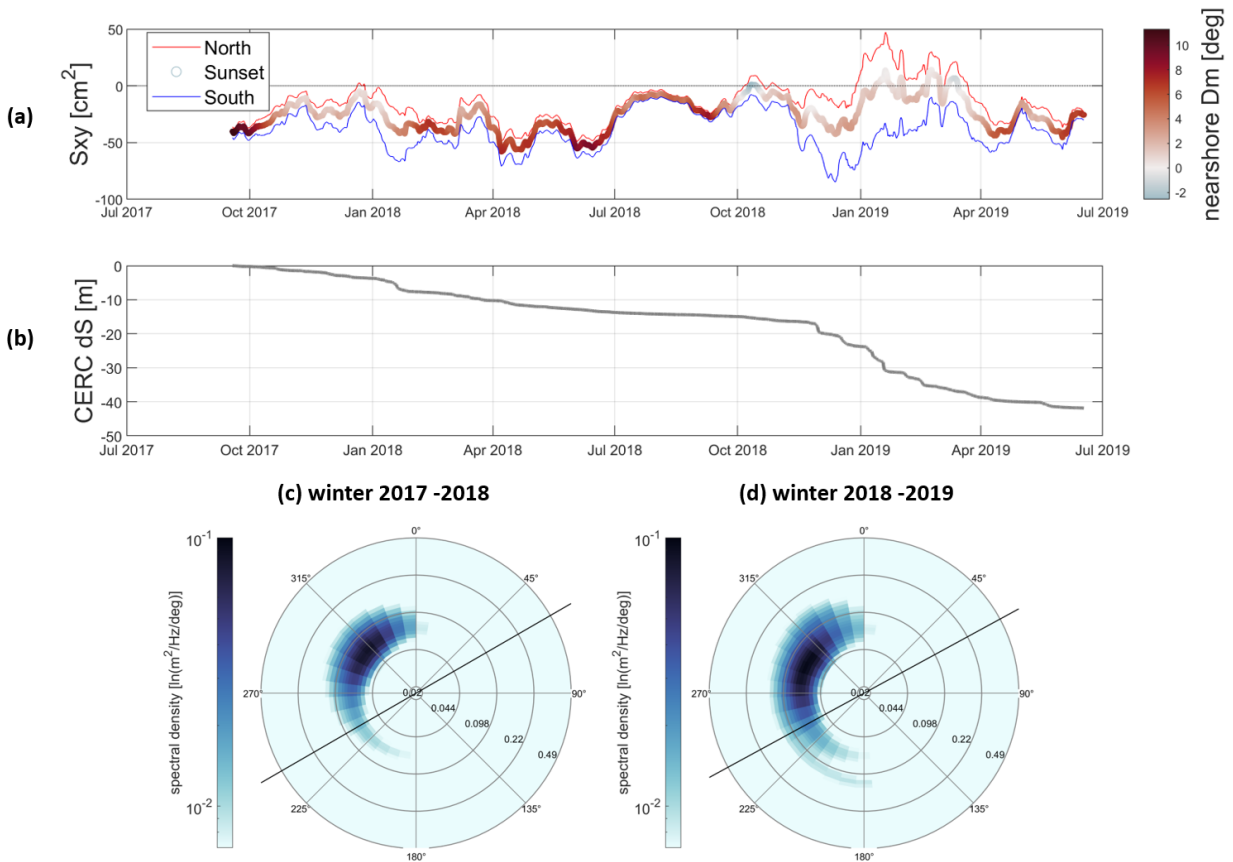
Figure 11: Panel (a) shows alongshore radiation stress (S_{xy}) 400m north of Sunset State Beach in red and 400m south in blue. Sunset S_{xy} is colored by CDIP MOP nearshore mean wave direction (Dm) relative to shore-normal: red colors are waves coming from the north and driving southward sediment transport. Panel (b) shows cumulative cross-shore shoreline change (*dS*) predicted by the CERC equation. Sediment transport was always negative (southward) between September 2017 and June 2019. Offshore spectral density and direction of offshore waves are shown in panels (c) and (d), outside of the Monterey submarine canyon system (from National Data Buoy Center station 46042). The black diagonal lines indicate the shoreline orientation Sunset State Beach. The rings of each polar plot represent wave frequencies, that range between 0.02 to 0.485 Hz, plotted on a log scale. Wave periods ranged between 4 to 23.5 seconds and spectral density ranged from 0 to 0.086 m^2/Hz/deg in winter 1 and 0 to 0.095 in winter 2. Mean spectral density was 3.5e^{-3} and 4.8e^{-3} m^2/Hz/deg in (c) and (d) respectively, while the median was 4.5e^{-4} and 8.9e^{-4}.

In the final modeling experiment, the equilibrium and CERC models were combined to estimate overall shoreline change due to cross- and alongshore sediment transport processes. During the 20-month time period, the combined shoreline change model achieved an RMSE of 5.6m, a modest improvement from the 6.4m RMSE by the equilibrium model alone. Every parameter changed slightly with the addition of the CERC equation, but all adjustments were within the ranges of parameter sensitivity (Table 3).

In the biannual time series, the shoreline erosion magnitude was variable from year to year and appeared to be partially forced by the average wave energy observed during periods of winter erosion, rather than a short-lived wave energy maximum (Table 5). For example, the highest waves on record in the Monterey Bay were observed in September 2017, but the winter of 2015-2016 had a greater average wave energy and corresponding shoreline erosion rate. Contrarily, the maximum amount of shoreline erosion was observed in 2018-2019 even though a moderate average wave energy was observed. Annual variability of the summer shoreline positions from 2014 – 2019 was not captured by any of the shoreline model experiments, as model predictions returned to approximately the same cross-shore position each year (Figure 12).

Table 5: Multivariate ENSO index (MEI.v2) for December/January of each winter are reported (ESRL NOAA). Red text = El Niño and blue text = La Niña winters. Significant wave height (Hs from CDIP MOP) was averaged while the shoreline was eroding. The erosion rate was defined as the cross-shore erosion in meters per day while the shoreline was eroding.

	2014 – 15	2015 – 16	2016 – 17	2017 – 18	2018 – 19
ENSO Index	0.2	**1.9**	-0.4	**-0.8**	0.1
Average Hs [m]	0.99	1.25	1.17	0.77	1.10
Erosion Rate [m/day]	-0.12	-0.29	-0.18	-0.05	-0.34
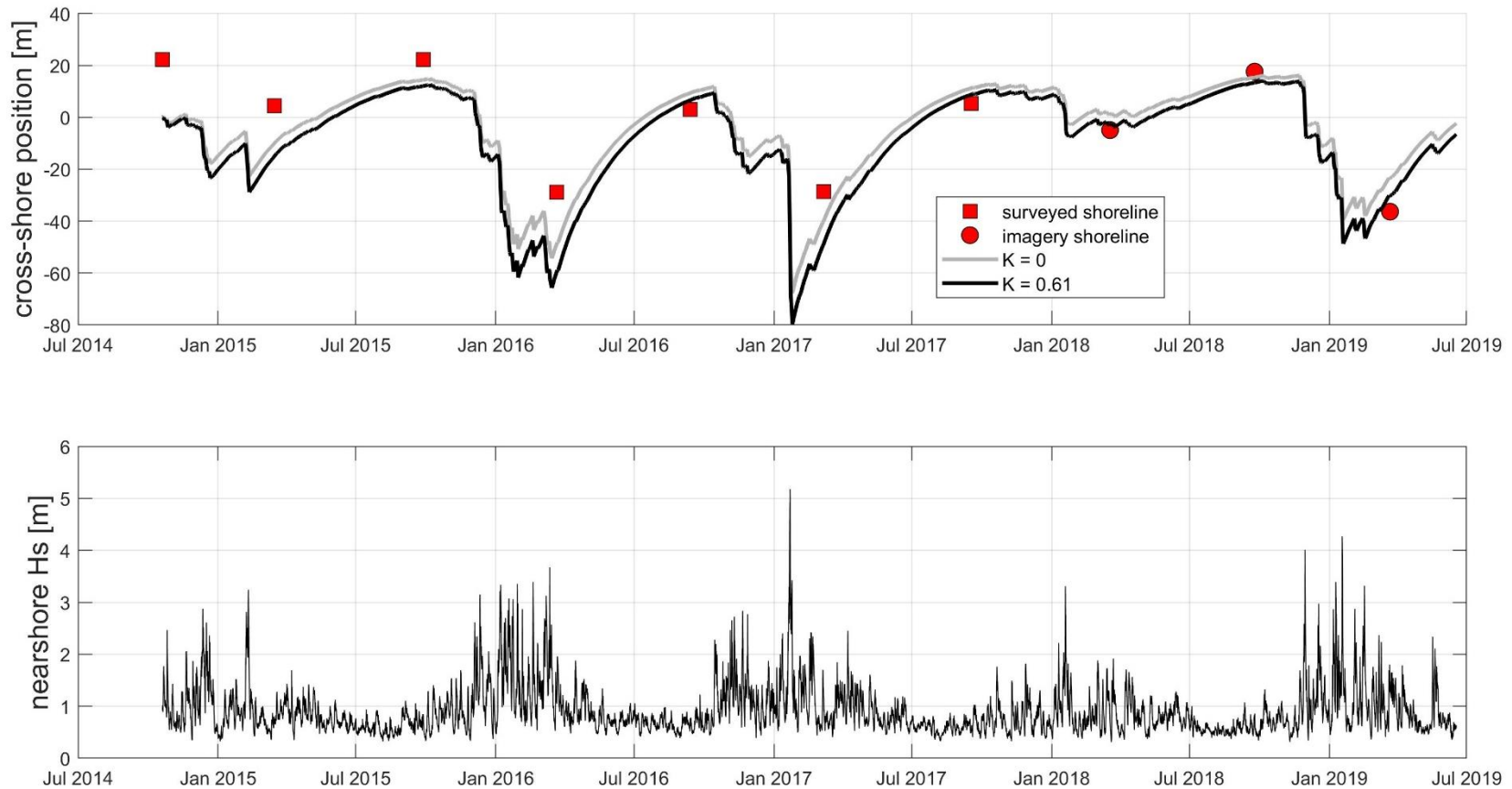
Figure 12: Biannual shoreline positions and nearshore significant wave height. The top panel shows biannual surveyed MHW shoreline positions (red boxes) (Stevens et al. 2017) extended with shorelines mapped using imagery (red circles). Biannual observations were extracted from the shorelines mapped using imagery in September and March of each year, following the sampling schedule of Stevens et al., (2017). The temporal mean was removed: positive positions correspond to accreted shorelines and negative positions correspond to eroded shorelines. The bottom panel shows hourly CDIP MOP nearshore significant wave height (Hs) from September 2014 to May 2019.

SECTION 4

DISCUSSION

The present study took place in Monterey Bay, where we investigated the effects of headland sheltering and complex inner shelf bathymetry on shoreline change at a sandy dune-backed beach, fronted by a submarine canyon system. The objectives of this study were twofold: 1) to define the relationships between shoreline and sandbar positions with wave conditions at the study site and 2) to test the drivers of shoreline change with simple shoreline change models. The drivers of shoreline change at Sunset State Beach are discussed in Section 4a, including a discussion of the role of the sandbar to shoreline change and wave impacts to sub-seasonal, seasonal, and interannual shoreline change. The sources and potential impacts of uncertainty in the results are examined in Section 4b and recommendations for future studies and coastal management are summarized in Section 4c.

4a. Drivers of Shoreline Change

In the first part of the study, the relationships between shoreline and sandbar positions were quantified to test the ability of the sandbar to delay winter shoreline erosion. Instead, the results suggest that a threshold in wave energy was the primary driver of early winter shoreline erosion. Nearshore significant wave heights exceeded the 95th percentile during the first storm event in the winter of 2017-2018 and 2018-2019, causing winter shoreline erosion to begin (Figure 6). The 95th percentile of wave height has been used to define storm events around the world and appears to be an accurate definition of storm events at the present study site (Harley et al., 2009, Angnuureng et al., 2017, Phillips et al., 2017). To better forecast future winter shoreline erosion, this results of the present study suggest that knowledge of the timing of the first storm of the winter that would drive waves over the 95th percentile in the nearshore could be helpful for accurate predictions of the timing of winter beach erosion.

High energy wave conditions were expected to drive rapid shoreline erosion. The results of this study suggest that a higher average winter wave energy drove more shoreline erosion than a short-lived energy maximum. The highest winter waves on record were recorded in 2017

offshore of the Monterey Bay, but did not drive enhanced shoreline erosion because the high wave event was much shorter in duration than the erosion timescale at Sunset State Beach (Table 4). The magnitude of shoreline erosion each year appeared to depend not only on average wave energy, but also the extent of shoreline recovery each summer. The largest magnitude of erosion was observed when the shoreline reached the maximum seaward position, observed in the winter of 2015-2016 and 2018-2019 (Table 5). The shoreline was also accreted in 2014-15, but the average wave energy was low so did not result in a high magnitude of erosion (Figure 11).

The results of this study further suggest that the sandbar aids summer shoreline accretion, rather than act to delay winter erosion. The shoreline eroded rapidly with high waves and accreted gradually with low waves, while the sandbar migrated both offshore and onshore gradually (Figure 9). These results agree with a study by Angnuureng et al. (2017), which suggests that shoreline recovery is primarily modulated by sandbar position according to a multiple linear regression. When wave conditions calm at the end of winter, the sandbar appears to become a source of sediment to replenish the eroded shoreline. This is true near Capitola, under 5km north of Seacliff State Beach, where the City of Capitola installs a nearshore sandbar in the early summer months to aid shoreline accretion (USACE et al., 2013). Further studies are required to conclude whether the presence of a sandbar delays winter erosion, but it is possible that the shoreline would have eroded sooner than was observed if the sandbar were not present at Sunset State Beach.

In the second part of the study, the results of the shoreline modeling experiments suggest that wave energy was the dominant driver of shoreline change at Sunset State Beach (Figures 10 & 11). Offshore waves that approached from the west in winter 2018-2019 increased the magnitude of winter shoreline erosion at Sunset State Beach, because they bypassed the Santa Cruz headlands and exposed the Monterey Bay to wave attack (Figure 12d). Though shoreline change due to alongshore sediment transport increased when offshore waves approached from the west, the RMSE of the combined equilibrium and CERC models was only modestly improved compared to the equilibrium shoreline change model alone (Table 3). We conclude that the influence of alongshore sediment transport is not a significant driver of shoreline change at Sunset State Beach. However, if this study were conducted in a different location within the Monterey Bay, we could have seen different results (Figure 13).

The alongshore wave energy gradient in the northern Monterey Bay becomes more pronounced in the winter, suggesting higher magnitudes of alongshore sediment transport north of latitude 36.9 and south of latitude 36.86 (Figure 13). CDIP MOP estimates of alongshore radiation stress, a proxy for sediment transport, suggest that shoreline change due to alongshore sediment transport may increase in the winter depending on the alongshore stretch of beach considered in calculations. Error in shoreline orientation and nearshore wave estimates are associated with CDIP MOP, so these estimates should be validated for accuracy (O'Reilly et al., 2016). Previous studies in the northern Monterey Bay have suggested erosion hotspots, which are attributed to the presence and migration of rip channels in the nearshore (Quan et al., 2013; Orzech et al., 2010). Our results suggest that erosion hotspots in the northern Monterey Bay could also be driven by wave refraction by the Monterey submarine canyon system.
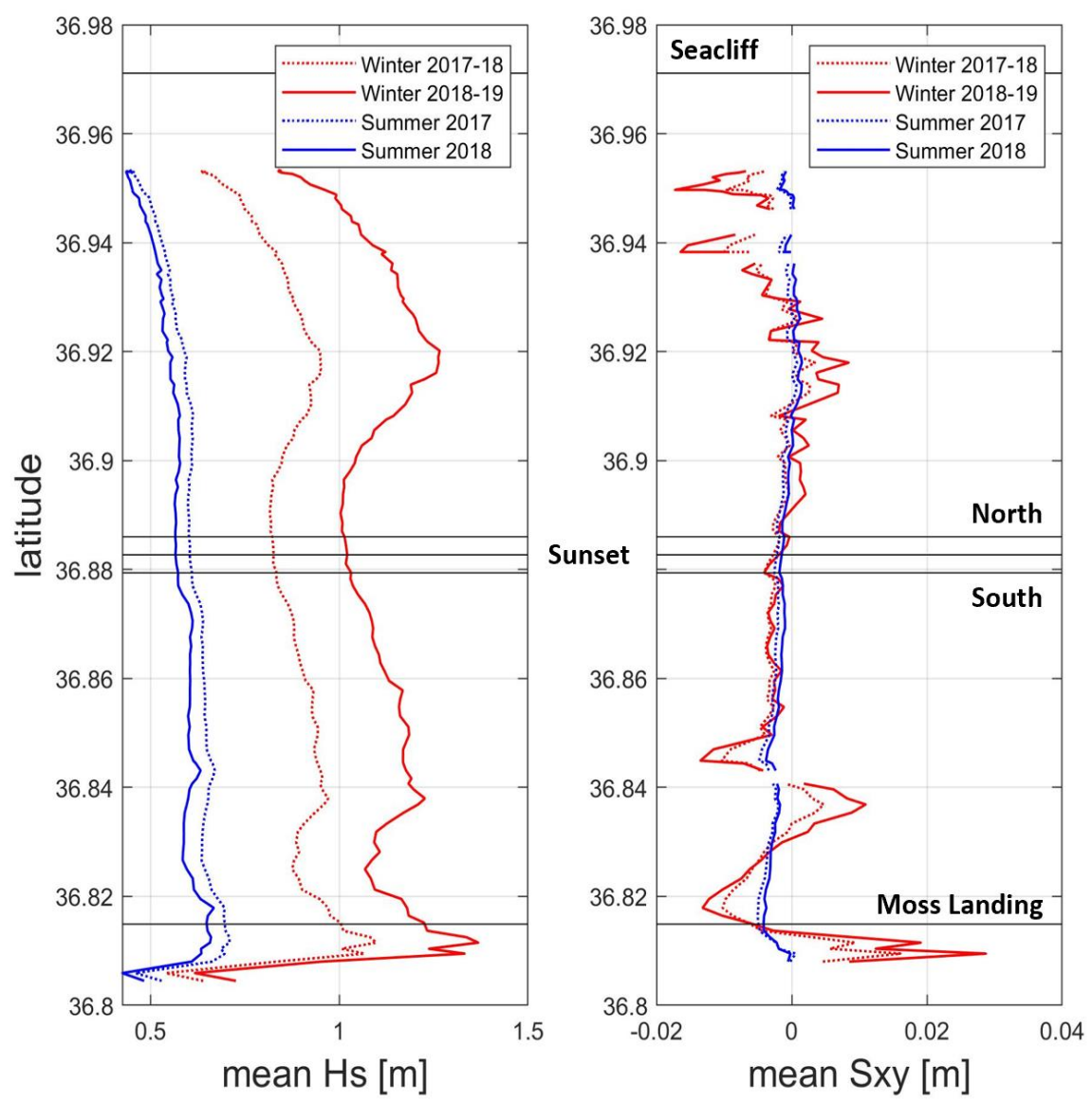
Figure 13: Averaged significant wave height (Hs) and alongshore radiation stress (Sxy) in the northern Monterey Bay. Winter (Nov, Dec, Jan) averages are shown in red and summer (Jul, Aug, Sep) averages in blue. The North and South horizontal lines denote the alongshore stretch of beach used to calculate shoreline change due to alongshore sediment transport in the present study.

The accuracy of the shoreline change models used in this study was limited by the annual variability in summer shoreline position (Figure 11). This contributes to the disparity in model skill between Sunset State Beach (RMSE = 6.4m) and the sites treated by Yates et al. (2009, 2011) (RMSE ~5m), because the sites treated by Yates et al. generally returned to the same cross-shore position each summer. The shoreline at Sunset State Beach appeared to take several years to recover after a highly erosive winter, agreeing with the findings of Dingler & Reiss (2002). The magnitude of winter shoreline erosion corresponded somewhat with interannual variability in average winter wave energy, associated with the El Niño Southern Oscillation, except during the winter 2018-2019 (Table 5).

During the winter of 2018-2019, offshore waves approached from the west and exposed the northern Monterey Bay to high energy wave conditions. Previous studies have shown that El Niño events drive high cliff and shoreline erosion in the Monterey Bay and west coast of the US (Barnard et al., 2017; Moore & Griggs, 2002; Quan et al., 2013; Thornton et al., 2006). North of the Sunset State Beach are sea cliffs, which if eroded during periods of high wave energy, could provide temporally variable pulses of sediment to the beach and nearshore. Such pulses of sediment could explain the annual variability in summer shoreline position, depending on the rate of alongshore sediment transport. In order to fully understand the influence of temporally variable sediment supply, the rate of sediment transport from the north of Sunset State Beach as well as the volume of sediment transported should be quantified.

The highest magnitudes of winter erosion at Sunset State Beach have historically occurred during El Niño years, when storm tracks tend to shift southward in the Pacific Ocean and expose the northern Monterey Bay to larger waves (Storlazzi & Griggs, 2000). The results of the present study show that high magnitudes of shoreline erosion can also occur during non- El Niño periods (Figure 12d). The high magnitude of shoreline erosion in 2015-2016 occurred during an El Niño period, but the high magnitude of shoreline erosion in 2018-2019, was during a non- El Niño period (Table 5). We suggest that rather than relying on predictions of an El Niño index to predict shoreline change, information regarding the direction of storm tracks could more accurately inform shoreline change predictions.

4b. Sources and Potential Impacts of Uncertainty

Video monitoring is subject to several sources of uncertainty that are discussed here but are not expected to have significantly altered the results of our study. Uncertainty associated with our results could have resulted from wave setup, the use of distant water levels in image rectification, and changes in still water level.

Wave setup occurs when momentum is transferred from wind to waves and then to shore (FEMA, 2005). Setup can cause water levels to be higher as they approach the shore depending on the level of momentum transfer, which increases with larger waves and steeper surf zones. Wave setup could act to displace the shoreline position landward, more than otherwise expected when only considering water levels outside of the surf zone, as we in the present study. Including estimates of nearshore setup to shoreline positions would likely result in shoreline position uncertainties upwards of 12m during high energy wave conditions (Angnuureng et al., 2017). Quantifying the amount of setup could help to identify a more accurate image rectification elevation to reduce uncertainty in morphologic mapping. Setup corrections were not applied in this study due to the lack of publicly available bathymetric data during the 20-month study period, at the time this study was conducted.

Further, the use of distant water levels during image rectification at Sunset State Beach may have added uncertainty to the mapped shoreline and sandbar positions. The maximum water level residual observed between the Monterey Tide Gauge and Seacliff State Beach, 10cm (Appendix 1), corresponds to a <1m cross-shore error according to beach profile surveyed in September 2017. This could have acted to displace the MHW shoreline at seaward by <1m at Sunset State Beach in August and October 2019, which contributed minimally to the overall uncertainty of shoreline positions. This displacement is expected to be higher in winter months, so further analysis of water level residuals during a variety of atmospheric and oceanographic conditions in the Monterey Bay will be necessary to fully quantify the uncertainty in shoreline and sandbar positions derived from imagery rectified to distant water levels.

Long-term sea level rise during the study period was minimal in the Monterey Bay. The estimated sea level rise trend calculated at the Monterey Tide Gauge is approximately 1.57 millimeters per year, summing to a five-year total of 7.85mm (NOAA Tides and Currents). However, the interannual variability in sea level due to changes in ocean temperature, periods of

upwelling vs. downwelling, atmospheric pressure, among other oceanographic properties, may be greater than the long-term trend. The uncertainty due to interannually variable sea level rise is unknown in terms of the present study but is expected to be on the order of centimeters according to Chelton & Davis (1982). Centimeters of variability in sea level will not have affected the shoreline mapping conducted in the present study, since 10cm results in a <1m cross-shore error.

4c. Recommendations for Future Studies

With continued work, Argus monitoring will improve our ability to forecast coastal change and has the potential to provide near-real time updates of coastal conditions, a valuable resource for coastal managers and communities. With improved projections of coastal change, communities can become proactive rather than reactive to the future of coastal change and increasing their resilience into the future of enhanced coastal hazards. Two worthwhile next steps are presented here.

The nearly 20-month time series of shoreline and sandbar positions highlights the utility of Argus monitoring stations. Such monitoring should be continued, but steps can be taken to reduce the manual effort in mapping shoreline and sandbar positions in order to provide near real-time updates of coastal morphology, in turn improving operational projections of coastal change. This has been accomplished in Australia, at the University of New South Wales' Water Research Laboratory, where researchers have automated the CCD shoreline mapping method and provide weekly updates of shoreline position to various interested coastal management groups. In Australia, the water is blue more of the time, where in the Monterey Bay, foggy and cloudy days inhibit this shoreline mapping method. Further exploration of the utility of different color channels should be explored to determine a more reliable CCD shoreline mapping method specific to the Monterey Bay and other grey areas around the world. It should also be possible to implement an automated sandbar mapping method, exploiting differences in pixel intensity in the nearshore. Sandbar mapping was done manually in this study, but some combination of image processing and thresholding would likely move us toward an automated workflow.

The performance of the equilibrium shoreline change model was likely influenced by time variable alongshore sediment flux. By quantifying alongshore sediment transport using

video imagery at Sunset State Beach, the contribution of alongshore processes could become clearer. This could be done using computer vision methods to track sequential migration of rip channels and other nearshore features at Sunset State Beach, suggesting a proxy for the magnitude of alongshore sediment transport in the style of Orzech et al. (2010). These estimates could then be compared to bulk alongshore sediment transport estimates using the Coastal Engineering and Research Center (CERC) formula to verify the results of this study (USACE 1984).

4d. Recommendations for Coastal Managers

The findings of this study inform resource management activities within the domain of NOAA's Monterey Bay National Marine Sanctuary (MBNMS). With sea level rise, local and regional management groups have formed to address the impacts of climate change to coastal communities (USACE et al., 2013). Two topics of current interest to coastal management are provided here, as well as how this study can inform their undertaking.

First, the last remaining sand mining plant in the U.S. is located in the southern Monterey Bay and has contributed to enhanced shoreline erosion in the area (Thornton et al., 2006). Due to public nuisance, the Monterey Bay community has voted for its closure in December of 2020 (California Coastal Commission, 2017). There is much interest in the region to monitor changes that are expected to occur following the sand plant's closure. Argus monitoring would provide an efficient means of monitoring coastal change around the sand mining plant to improve our understanding of the impact of coastal sand mining to downcoast communities. Given the strong community interest, Argus monitoring has the potential to provide rapid updates to community members, which would be difficult to provide using traditional survey methods that are time intensive.

Second, the Monterey community has been considering the installation of a coastal water desalination plant to help alleviate water shortages in the area. This involves the installation of a nearshore intake pipe to draw seawater from near the coast into residential areas. This study reveals rapid shoreline migration that occurs up to 350 meters away from the dune crest. Consideration to the placement of the desalination intake pipe should be given to the cross-shore

range of sandbar migration, so that the intake pipe does not get obstructed by rapidly moving sand in the nearshore zone.

SECTION 5

CONCLUSIONS

The present study took place in Monterey Bay, where we investigated the relationships between shoreline and sandbar positions with wave conditions, and the influence of cross-and alongshore sediment transport to shoreline change. The effects of headland sheltering and complex inner shelf bathymetry on shoreline change at a sandy dune-backed beach, fronted by a submarine canyon system were investigated using video monitoring, in-situ surveys, and simple shoreline change models.

We observed that winter shoreline erosion occurred once nearshore significant wave heights exceeded 1.7m, the 95th percentile. Rather than delay winter shoreline erosion, the sandbar aided in shoreline recovery as it migrated onshore gradually, corresponding with gradual shoreline accretion. The shoreline eroded rapidly during high energy wave conditions and accreted gradually with low energy wave conditions, exhibiting an equilibrium shoreline response. The duration of high energy wave events or storms in the winter corresponded with higher shoreline erosion magnitudes, where higher average winter wave energy drove higher magnitudes of shoreline erosion.

A simple equilibrium model represented shoreline change at Sunset State Beach. Model predictions of shoreline position were not significantly improved by the addition of an alongshore sediment transport term. We conclude that the primary driver of shoreline change at the study site is wave energy, which was observed to increase when the offshore waves approached from the west. The southward shift in wave direction resulted in reduced sheltering by the Santa Cruz headlands, exposing the northern Monterey Bay to increased wave attack. Shoreline change model performance was degraded by annual variability in the summertime shoreline position, which may be influenced by temporally variable alongshore sediment supply. We suggest that rather than relying on predictions of an El Niño index to predict shoreline change, information regarding the direction of storm tracks could more accurately inform shoreline change predictions.

APPENDIX 1

WATER LEVELS IN MONTEREY BAY

A radar water level sensor was installed at Seacliff State Beach, approximately 10km north of the Sunset State Beach (Figure 14), to quantify uncertainty in shoreline and sandbar positions extracted from imagery rectified to distant datum elevations. The Nile 502 sensor collected water level measurements once per second and reported the 6-minute averaged water level during all hours of the day. It was hypothesized that local wind driven setup from the south to north Monterey Bay, or vice versa, may drive variations in water level. South to north wave setup could cause higher water levels in the northern Monterey Bay than those observed in the south with southerly winds, for example. Previous studies similarly lacking a nearby tide gauge have used tide models or pressure sensors in the nearshore to estimate local water levels (Angnuureng et al., 2017; Stokes et al., 2015). Considering the bathymetric variability, semi-enclosed geography, and lack of previous measurements of water levels in the northern Monterey Bay, we chose to install a radar water level sensor nearby Sunset State Beach.

Tide gauges around the U.S. are historically in-water acoustic sensors, upkept by the National Oceanic and Atmospheric Administration (NOAA). Interestingly, NOAA is moving toward using radar water level sensors in their tide monitoring network across the U.S. to reduce servicing effort and cost, so has begun testing radar water level sensors like the one installed at Seacliff State Beach against the historic acoustic sensors. According to tests between similar models of acoustic and radar sensors in semi-enclosed coastal regions, NOAA determined that 6-minute measurements collected concurrently were comparable within 1cm, encouraging the use of a radar sensor in the present study (Heitsenrether & Davis, 2011).

The sensor was installed at Seacliff State Beach in August 2019, outside of the surf zone, to maintain comparability to the Monterey tide gauge. The pier at Seacliff was the closest structure extending outside of the nearshore to Sunset State Beach at the time of this study. To ensure that the sensors at Seacliff and Monterey were referenced to the same vertical datum and water levels were directly comparable, both sensors were surveyed concurrently using a static GPS for four hours following the Seacliff sensor installation in August 2019. Preliminary results comparing water levels between Seacliff and Monterey suggest diurnal fluctuations in water level residuals, as well as more sustained residuals during the week of August 22 and in late

September 2019 (Figure 15). Further analysis of water level residuals will be necessary to fully quantify error; it is expected that residuals between the north and south will diverge the most during the winter when local winds are high.

Figure 14: Radar water level sensor at Seacliff State Beach.
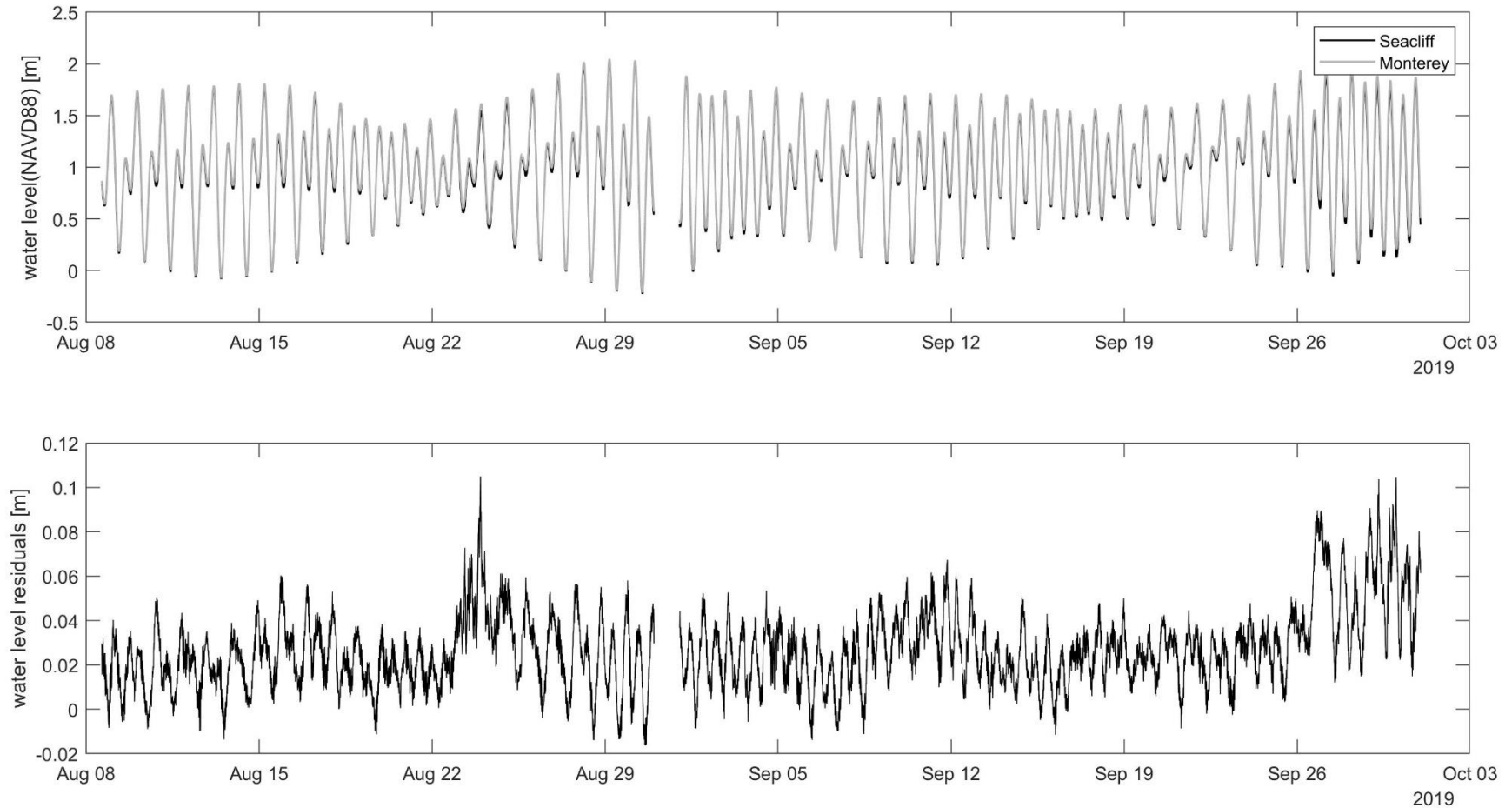
Figure 15: Comparison between total water levels at Seacliff State Beach and the Monterey Wharf. Water levels in the top panel are georeferenced to NAVD88; a 0m water level corresponds to the elevation of NAVD88. Positive residuals in the bottom panel indicate times when the Monterey tide gauge reported higher water levels than those in Seacliff. GPS surveying and data processing was performed by Joshua Logan of USGS.

REFERENCES

Andriolo, U. (2019). Nearshore Wave Transformation Domains from Video Imagery. Journal of Marine Science and Engineering, 7(6), 186. https://doi.org/10.3390/jmse7060186

Angnuureng, D. B., Almar, R., Senechal, N., Castelle, B., Addo, K. A., Marieu, V., & Ranasinghe, R. (2017). Shoreline resilience to individual storms and storm clusters on a meso-macrotidal barred beach. Geomorphology, 290(August 2015), 265–276. https://doi.org/10.1016/j.geomorph.2017.04.007

Barnard, P. L., Hoover, D., Hubbard, D. M., Snyder, A., Ludka, B. C., Allan, J., Serafin, K. A. (2017). Extreme oceanographic forcing and coastal response due to the 2015-2016 El Niño. Nature Communications, 8, 1–8. https://doi.org/10.1038/ncomms14365

Blossier, B., Bryan, K. R., Daly, C. J., & Winter, C. (2017). Shore and bar cross-shore migration, rotation, and breathing processes at an embayed beach. Journal of Geophysical Research: Earth Surface, 122 (10), 1745–1770. https://doi.org/10.1002/2017JF004227

Burvingt, O., Masselink, G., Russell, P., & Scott, T. (2017). Classification of beach response to extreme storms. Geomorphology, 295, 722–737. https://doi.org/10.1016/j.geomorph.2017.07.022

Buscombe, D., Harrison, S. R., & Warrick, J. A. (2020, February). Optical nearshore wave gauging with deep neural networks. In *Ocean Sciences Meeting 2020*. AGU.

Camenen, B., & Larson, M. (2007). Predictive Formulas for Breaker Depth Index and Breaker Type. Journal of Coastal Research, 234(234), 1028–1041. https://doi.org/10.2112/05-0566.1

Chelton, D. B., & Davis, R. E. (1982). Monthly mean sea-level variability along the west coast of North America. *Journal of Physical Oceanography*, *12*(8), 757-784.California Coastal Commission, (2017). CCC-17-CD-02 CEMEX Cease and Desist Order CCC-17-CD-02.

Coco, G., Senechal, N., Rejas, A., Bryan, K. R., Capo, S., Parisot, J. P., MacMahan, J. H. M. (2014). Beach response to a sequence of extreme storms. Geomorphology, 204, 493–501. https://doi.org/10.1016/j.geomorph.2013.08.028

Crosby, S. C., O'Reilly, W. C., & Guza, R. T. (2016). Modeling long-period swell in Southern California: Practical boundary conditions from buoy observations and global wave model predictions. Journal of Atmospheric and Oceanic Technology, 33(8), 1673–1690. https://doi.org/10.1175/JTECH-D-16-0038.1

Davidson, M. A., Splinter, K. D., & Turner, I. L. (2013). A simple equilibrium model for predicting shoreline change. Coastal Engineering, 73, 191–202. https://doi.org/10.1016/j.coastaleng.2012.11.002

Dingler, J. R., & Reiss, T. E. (2002). Changes to Monterey Bay beaches from the end of the 1982-83 El Niño through the 1997-98 El Niño. Marine Geology, 181(1–3), 249–263. https://doi.org/10.1016/S0025-3227(01)00270-5

Erikson, L. H., Storlazzi, C. D., & Golden, N. E. (2014). Modeling Wave and Seabed Energetics on the California Continental Shelf. https://doi.org/10.5066/F7125QNQ.2014

ESRL NOAA, accessed January 2019.
https://tidesandcurrents.noaa.gov/sltrends/sltrends_station.shtml?id=9413450

FEMA, (2005). Guidelines and Specifications for Flood Hazard Mapping Partners, D.4.5 Wave Setup, Runup, and Overtopping. Retrieved from https://www.fema.gov/media-library-data/d5628f66b0b3189e0891e0c1a580a013/Wave+Setup+Runup+and+Overtopping+-+Chapter-Section+Number+-+D.4.5.pdf

Glover, D. M., Jenkins, W. J., & Doney, S. C. (2011). *Modeling methods for marine science*. Cambridge University Press.

Griggs, G., & Patsch, K. (2007). Development of Sand Budgets for California's Major Littoral Cells. Book.

Hapke, C. J., Plant, N. G., Henderson, R. E., Schwab, W. C., & Nelson, T. R. (2016). Decoupling processes and scales of shoreline morphodynamics. Marine Geology, 381, 42–53. https://doi.org/10.1016/j.margeo.2016.08.008

Harley, M.D., Turner, I.L., Short, A.D., Ranasinghe, R., 2009. An empirical model of beach response to storms-SE Australia. Coasts and Ports 2009: in a Dynamic Environment, p. 600.

Harley, M.D., accessed May 2018. Shoreline Mapping Toolbox. https://github.com/Coastal-Imaging-Research-Network/Shoreline-Mapping-Toolbox

Harrison, S. R., Bryan, K. R., & Mullarney, J. C. (2017). Observations of morphological change at an ebb-tidal delta. *Marine Geology*, *385*, 131-145.

Heitsenrether, R., & Davis, E. (2011). Test and evaluation report, Limited acceptance of the design analysis WaterLog H-3611i microwave radar water level sensor. NOAA Technical Report NOS CO-OPS061, Ocean Systems Test and Evaluation Program, (March).

Hoefel, F., & Elgar, S. (2003). Wave-Induced Sediment Transport and Sandbar Migration. Science, 299(March), 1885–1887.

Holman, R. A., & Stanley, J. (2007). The history and technical capabilities of Argus. Coastal Engineering, 54(6–7), 477–491. https://doi.org/10.1016/j.coastaleng.2007.01.003

Komar, P. D., & Inman, D. L. (1970). Longshore Sand Transport on Beaches in and near and compute and spectra [Koontz and p are . respectively the sand and tools began in 1966 . In a preliminary report for pore space and can be taken It is Inman verified that the longshore advantageous to ex, 75(30), 5914–5927.

Lippmann, T. C., & Holman, R. A. (1989). Quantification of sand bar morphology: a video technique based on wave dissipation. Journal of Geophysical Research, 94(C1), 995–1011. https://doi.org/10.1029/JC094iC01p00995

Lippmann, T. C., & Holman, R. A. (1990). The spatial and temporal variability of sand bar morphology. Journal of Geophysical Research, 95(C7), 11575. https://doi.org/10.1029/JC095iC07p11575

Mentaschi, L., Vousdoukas, M. I., Voukouvalas, E., Dosio, A., & Feyen, L. (2017). Global changes of extreme coastal wave energy fluxes triggered by intensified teleconnection patterns. Geophysical Research Letters, 44(5), 2416–2426. https://doi.org/10.1002/2016GL072488

Moore, L. J., & Griggs, G. B. (2002). Long-term cliff retreat and erosion hotspots along the central shores of the Monterey Bay National Marine Sanctuary. Marine Geology, 181(1–3), 265–283. https://doi.org/10.1016/S0025-3227(01)00271-7

Moore, L. J., Ruggiero, P., & List, J. H. (2006). Comparing Mean High Water and High Water Line Shorelines: Should Proxy-Datum Offsets be Incorporated into Shoreline Change Analysis? Journal of Coastal Research, 224(4), 894–905. https://doi.org/10.2112/04-0401.1

Munk, W. H., & Traylor, M. A. (1947). Refraction of Ocean Waves: A Process Linking Underwater Topography To Beach Erosion. The Journal of Geology, 55(1), 1–26.

Neumann, J. E., Emanuel, K., Ravela, S., Ludwig, L., Kirshen, P., Bosma, K., & Martinich, J. (2014). Joint effects of storm surge and sea-level rise on US Coasts: new economic estimates of impacts, adaptation, and benefits of mitigation policy. Climatic Change, 129(1–2), 337–349. https://doi.org/10.1007/s10584-014-1304-z

O'Reilly, W. C., Olfe, C. B., Thomas, J., Seymour, R. J., & Guza, R. T. (2016). The California coastal wave monitoring and prediction system. Coastal Engineering, 116, 118–132. https://doi.org/10.1016/j.coastaleng.2016.06.005

Phillips, M. S., Harley, M. D., Turner, I. L., Splinter, K. D., & Cox, R. J. (2017). Shoreline recovery on wave-dominated sandy coastlines: the role of sandbar morphodynamics and nearshore wave parameters. Marine Geology, 385, 146–159. https://doi.org/10.1016/j.margeo.2017.01.005

Plant, N. G., Aarninkhof, S. G. J., Turner, I. L., & Kingston, K. S. (2007). The Performance of Shoreline Detection Models Applied to Video Imagery. Journal of Coastal Research, 233(3), 658–670. https://doi.org/10.2112/1551-5036(2007)23[658:TPOSDM]2.0.CO;2

Quan, S., Kvitek, R. G., Smith, D. P., & Griggs, G. B. (2013). Using Vessel-Based LIDAR to Quantify Coastal Erosion during El Niño and Inter-El Niño Periods in Monterey Bay, California. Journal of Coastal Research, 288, 555–565. https://doi.org/10.2112/JCOASTRES-D-12-00005.1

Semedo, A., Weisse, R., Behrens, A., Sterl, A., Bengtsson, L., & Günther, H. (2013). Projection of global wave climate change toward the end of the twenty-first century. Journal of Climate, 26(21), 8269–8288. https://doi.org/10.1175/JCLI-D-12-00658.1

Senechal, N., Coco, G., Castelle, B., & Marieu, V. (2015). Storm impact on the seasonal shoreline dynamics of a meso- to macrotidal open sandy beach (Biscarrosse, France). Geomorphology, 228(January), 448–461. https://doi.org/10.1016/j.geomorph.2014.09.025

Splinter, K. D., Carley, J. T., Golshani, A., & Tomlinson, R. (2014). A relationship to describe the cumulative impact of storm clusters on beach erosion. Coastal Engineering, 83, 49–55. https://doi.org/10.1016/j.coastaleng.2013.10.001

Splinter, K. D., Turner, I. L., Davidson, M. A., Barnard, P., Castelle, B., & Oltman-Shay, J. (2014). A generalized equilibrium model for predicting daily to inter-annual shoreline response A generalized equilibrium model for predicting daily to inter-annual shoreline response. Journal of Geophysical Research: Earth Surface, 119, 1936–1958. https://doi.org/10.1002/2014JF003106

Stevens, A.W., Logan, J.B., Snyder, A.G., Hoover, D.J., Barnard, P.L., Warrick, J.A., 2017, Beach topography and nearshore bathymetry of northern Monterey Bay, California: U.S. Geological Survey data release, https://doi.org/10.5066/F76H4GCW.

Stive, M. J. F., Aarninkhof, S. G. J., Hamm, L., Hanson, H., Larson, M., Wijnberg, K. M., … Capobianco, M. (2002). Variability of shore and shoreline evolution. Coastal Engineering, 47(2), 211–235. https://doi.org/10.1016/S0378-3839(02)00126-6

Stokes, C., Davidson, M., & Russell, P. (2015). Observation and prediction of three-dimensional morphology at a high-energy macrotidal beach. Geomorphology, 243, 1–13. https://doi.org/10.1016/j.geomorph.2015.04.024

Storlazzi, C. D., & Griggs, G. B. (2000). Influence of El Niño-Southern Oscillation (ENSO) events on the evolution of Central California's shoreline. Bulletin of the Geological Society of America, 112(2), 236–249. https://doi.org/10.1130/0016-7606(2000)112<236:IOENOE>2.0.CO;2

Thornton, E. B., Sallenger, A., Sesto, J. C., Egley, L., McGee, T., & Parsons, R. (2006). Sand mining impacts on long-term dune erosion in southern Monterey Bay. Marine Geology, 229(1–2), 45–58. https://doi.org/10.1016/j.margeo.2006.02.005

USACE, 1984. Shore Protection Manual. Department of the Army, U.S. Corps of Engineers, Washington, DC 20314.

USACE, MBNMS, & Noble Consultants. (2013). Coastal Regional Sediment Management Plan for the Santa Cruz Littoral Cell, Pillar Point to Moss Landing.

USGS, (2017). Accessed January 2019. Eyes on the Coast—Video Cameras Help Forecast Coastal Change. https://www.usgs.gov/center-news/eyes-coast-video-cameras-help-forecast-coastal-change?qt-news_science_products=1#qt-news_science_products

van Enckevort, I. M. J., & Ruessink, B. G. (2001). Effect of hydrodynamics and bathymetry on video estimates of nearshore sandbar position. Journal of Geophysical Research, 106(16), 969–979.

Vitousek, S., Barnard, P. L., Limber, P., Erikson, L., & Cole, B. (2017). A model integrating longshore and cross-shore processes for predicting long-term shoreline response to climate change. Journal of Geophysical Research: Earth Surface, 122(4), 782–806. https://doi.org/10.1002/2016JF004065

Wright, L. D., & Short, A. D. (1984). Morphodynamic variability of surf zones and beaches: A synthesis. Marine Geology, 56(1–4), 93–118. https://doi.org/10.1016/0025-3227(84)90008-2

Yates, M. L., Guza, R. T., & O'Reilly, W. C. (2009). Equilibrium shoreline response: Observations and modeling. Journal of Geophysical Research: Oceans, 114(9), 1–16. https://doi.org/10.1029/2009JC005359

Yates, M. L., Guza, R. T., O'Reilly, W. C., Hansen, J. E., & Barnard, P. L. (2011). Equilibrium shoreline response of a high wave energy beach. *Journal of Geophysical Research: Oceans*, *116*(C4).

Zhang, K. Q., Douglas, B. C., & Leatherman, S. P. (2004). Global warming and coastal erosion. Climatic Change, 64(1–2), 41–58. https://doi.org/10.1023/b:clim.0000024690.32682.48